

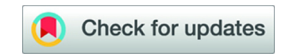
Online: ISSN 2008-949X

# **Journal of Mathematics and Computer Science**



Journal Homepage: www.isr-publications.com/jmcs

# Mathematical modeling and optimal control strategies for COVID-19: insights from initial public interventions in Thailand



Chairat Modnak<sup>a,\*</sup>, Adison Thongtha<sup>b</sup>, Pattarapan Kumpai<sup>c</sup>

#### **Abstract**

Since 2020, Thailand has been actively combating the COVID-19 pandemic. Initially, the country faced a significant surge in infections but has since adapted its strategies to manage the virus more effectively. During the fourth wave in 2021, Thailand categorized its population into eight groups: susceptible individuals, exposed, and infectious individuals, those treated in field hospitals, individuals receiving ICU care without oxygen support, those in ICU with oxygen support, individuals in critical condition, recovered individuals, and the deceased. Treatment in field hospitals is considered equivalent to care in standard hospitals. We aim to gain insight into the dynamics of the disease to better prepare for similar diseases in the future. To achieve this, we developed a mathematical framework consisting of eight differential equations, grounded in fundamental mathematical principles. We calculated the reproduction number and analyzed the initial intervention strategies implemented by the Thailand Public Health Administration. Numerical simulations of the optimal control problem highlight the critical role of preventing exposed and infectious individuals from infecting the susceptible population in curbing COVID-19 transmission. Additionally, our optimal control simulation indicates that vaccination policies should aim to inoculate approximately 46 percent (rather that 70 percent) of the population (at a daily rate of 0.2 percent) within the first 230 days of an outbreak to effectively halt disease transmission. However, this result is based on certain assumptions in the model simulations, and the outbreak was not the first wave. Therefore, the public health intervention program should be implemented as broadly as possible to cover the population effectively.

**Keywords:** Mathematical modeling, Covid-19, infectious disease modeling, optimal control study, COVID-19 Thailand modeling.

2020 MSC: 92B05, 37N25, 34D20.

©2026 All rights reserved.

#### 1. Introduction

Thailand recorded its first COVID-19 case on January 13, 2020, with cases steadily increasing throughout February and March. In response, Thai public health authorities swiftly implemented intervention

Email addresses: chairatm@nu.ac.th (Chairat Modnak), adison7595@gmail.com (Adison Thongtha), pattarapan.k@mdes.go.th (Pattarapan Kumpai)

doi: 10.22436/jmcs.041.02.02

Received: 2025-07-01 Revised: 2025-07-30 Accepted: 2025-08-14

<sup>&</sup>lt;sup>a</sup>Department of Mathematics, Faculty of Science, Naresuan University, Phitsanulok, 65000, Thailand.

<sup>&</sup>lt;sup>b</sup>Energy Policy and Planning Office, Ministry of Energy, Bangkok, 10400, Thailand.

<sup>&</sup>lt;sup>c</sup>Ministry of Digital Economy and Society (MDES), the Government Complex, Bldg. C, Chaeng Watthana Rd., Laksi, Bangkok, 10210, Thailand.

<sup>\*</sup>Corresponding author

measures, including social distancing protocols, mandatory mask-wearing mandates, and the closure of schools. Additionally, infected individuals were hospitalized, while those exposed to the virus were mandated to undergo a 14-day quarantine period [38].

The initial surge of COVID-19 cases in Thailand was largely linked to an outbreak at a boxing stadium in Bangkok and various entertainment venues. In response, the government enacted stringent measures, including nationwide lockdowns, business closures, curfews, and travel restrictions. As the situation gradually improved after the first wave, restrictions were eased, with authorities shifting their focus to extensive testing, contact tracing, and case isolation to manage outbreaks effectively. Nonetheless, sporadic clusters continued to emerge, prompting localized lockdowns and targeted interventions to curb further spread [38].

Throughout 2020, Thailand recorded relatively fewer COVID-19 cases than many other countries, a result of swift containment measures such as travel restrictions, mandatory quarantines, and lockdowns. Despite these efforts, several waves occurred, particularly during the early months and towards the end of the year, bringing the total case count into the tens of thousands [8].

In 2021, the emergence of the Delta variant triggered Thailand's fourth wave, beginning in late March. Daily infections peaked at around 25,000 in mid-September before declining to approximately 2,000 per day by early January 2022 [10].

The year 2022 marked a significant shift in strategy, as Thailand moved towards reopening and transitioning from a pandemic to an endemic management approach. Although detailed data are unavailable, it is presumed that case numbers increased compared to 2021 due to the spread of the Omicron variant. As of May 2024, Thailand had reported a cumulative total of 4,770,149 confirmed cases, with a considerable proportion likely occurring in 2022 [9]. A notable policy change occurred in September 2022, when the Emergency Decree related to COVID-19 was lifted, and the disease was reclassified from a "dangerous communicable disease" to a "communicable disease under surveillance," aligning its management with other endemic illnesses [9].

In 2023, the country's focus shifted towards living with the virus, with fewer restrictions and greater emphasis on economic recovery. However, by 2024, Thailand began facing a renewed resurgence of COVID-19 cases. Since March 2024, there has been a sustained rise in hospitalizations, severe cases, and fatalities. Weekly reports from the Ministry of Public Health indicate a consistent upward trend, with the most recent data showing 1,672 new admissions and nine fatalities in the past week alone. Among these, 390 patients were classified as severely ill, and 148 required mechanical ventilation as of April 27. While there is no evidence suggesting that the current variants cause more severe disease, the escalation is likely driven by higher transmissibility of circulating strains and reduced adherence to personal protective measures, particularly during the Songkran festivities [10].

Thailand initiated its COVID-19 vaccination program on February 28, 2021, administering the CoronaVac vaccine to individuals aged 18-59, followed by the AstraZeneca vaccine for those aged 60 and above on March 16, 2021. The Sinopharm vaccine became available to the general population on June 25, 2021, with the Pfizer vaccine introduced in limited quantities on August 9, 2021, and the Moderna vaccine on November 1, 2021. From January 2022, the vaccination program was expanded to include booster doses. By October 2022, COVID-19 was officially reclassified in Thailand as a communicable disease under surveillance [8].

Between 2021 and 2022, Thailand progressively adapted its COVID-19 management strategies, shifting towards reopening and learning to coexist with the virus. Treatment protocols evolved to prioritize home isolation or care in field hospitals for mild cases, reserving hospital beds for severe infections. Individuals with mild symptoms and no underlying health conditions were encouraged to quarantine at home under medical guidance. For those requiring closer monitoring or facing difficulties in isolation, care was provided in field hospitals, often located in repurposed hotels or large tents equipped to deliver basic medical services. These approaches contributed to a noticeable decline in new infections. Building on these public health measures, the present study seeks to develop a mathematical model tailored to Thailand's specific interventions [8].

According to the World Health Organization (WHO) [10], global SARS-CoV-2 activity has been rising since mid-February 2025, with test positivity reaching 11 %-a level last observed in July 2024. The resurgence is most pronounced in the Eastern Mediterranean, South-East Asia, and Western Pacific regions. Early 2025 also brought a slight shift in variant trends, with a Variant Under Monitoring (VUM) accounting for 10.7 % of reported sequences by mid-May, echoing patterns from the same period the previous year. Vaccination remains central to global control efforts, preventing severe disease and death, particularly among high-risk populations.

Given our emphasis on mathematical modeling with optimal control, this review focuses on the development and analysis of epidemic models and their associated control strategies. In 2020, Liu et al. [22] examined the latent period before infectiousness, proposing two differential equation models-one grouping exposed individuals with the infected class, and another introducing a transmission delay-applied to COVID-19 data from China to estimate parameters such as transmission rate and reproduction number. Their work highlighted the influence of unreported cases and the importance of public health interventions.

Also in 2020, Zhao and Chen [44] proposed the SUQC model (susceptible, un-quarantined infected, quarantined infected) to evaluate the impact of intervention measures in China. While demonstrating the benefits of quarantine, it did not explore other control options. That year, Mahajan et al. [24] developed the SIPHERD model (susceptible, exposed, symptomatic, purely asymptomatic, hospitalized/quarantined, recovered, deceased) to project confirmed cases, active cases, and deaths. They found that enhanced testing, strict social distancing, and timely lockdowns could significantly reduce transmission, even without vaccines.

In 2021, Rajput et al. [36] modeled transmission in India across eight population groups, including vaccinated individuals, undetected infectives, and hospitalized cases. They concluded that prioritizing vaccination for exposed and undetected infectives-while lowering rates for susceptibles-could sustain control while reducing costs. That same year, Lu et al. [23] proposed a two-stage epidemic model for China that integrated dynamic control strategies to minimize costs while maintaining societal function, proving effective during the second wave.

In 2022, Misra et al. [25] developed a model incorporating hospital bed availability with a time delay to reflect capacity expansion, emphasizing the critical role of increasing capacity during surges. That year, Dhar et al. [13] introduced a fractional-order SEVR model, demonstrating that even partial vaccination can provide delayed but meaningful benefits. By 2023, modeling efforts had expanded to address policy fluctuation impacts (Vallee et al. [40]), quarantine integration into SEIQRD frameworks (Darti et al. [11]), and the effects of vaccination stages on outbreak dynamics (Aakash et al. [1]). Additional studies examined screening and treatment in typhoid fever [17], infective immigration in rabies spread [28], and equilibrium stability in SEIR-based COVID-19 models [1].

Researches in 2024 further diversified, incorporating stochasticity into deterministic models [5], analyzing discrete-time epidemic frameworks [15], and studying delayed optimal control interventions [21]. Other work addressed behavioral changes and Allee effects in SEIQRD structures [1], cost-effectiveness in combined COVID-19 control measures [30], and vector control strategies for dengue fever [27].

In 2025, studies broadened beyond COVID-19, including malnutrition's influence on tuberculosis [20], fractional-order rabies models with memory effects [32], optimal control in rabies culling and vaccination [26], and intervention analysis for Marburg virus [31], norovirus [33], and conjunctivitis [29].

Collectively, these contributions provide essential guidance for constructing our own model of COVID-19 transmission in Thailand. We begin by collecting and analyzing national case data, then develop a novel model reflecting local dynamics. We calculate the basic reproduction number, analyze equilibrium stability, and perform sensitivity analysis to identify key parameters. Optimal control strategies are then evaluated through simulations comparing no intervention, single measures, and combined approaches against real-world data. The results inform public health recommendations aimed at supporting more effective COVID-19 policies in Thailand.

#### 2. Mathematical model

We began by analyzing COVID-19 data from the Thai Public Health Administration for 2021, which served as the foundation for constructing our mathematical model. The population is divided into eight compartments: susceptible individuals (S); exposed and infectious individuals (E); infectious individuals receiving treatment in field hospitals ( $I_1$ ); those treated in the ICU without oxygen support ( $I_2$ ); patients in the ICU with oxygen support ( $I_3$ ); individuals in critical condition ( $I_4$ ); recovered individuals (R); and deceased individuals (D).

Susceptible individuals become infected through close contact with infectious individuals from various classes, with transmission rates denoted as  $\beta_1$  (from those in field hospitals),  $\beta_2$  (from ICU patients without oxygen),  $\beta_3$  (from ICU patients with oxygen), and  $\beta_4$  (from exposed infectious individuals). The natural birth and death rate is represented by  $\mu$ , while  $\Lambda$  denotes the recruitment rate of the population. Exposed individuals progress to symptomatic infection at rates  $\alpha_1$ ,  $\alpha_2$ ,  $\alpha_3$ , and  $\alpha_4$ , corresponding to the different infectious classes. COVID-19-related death rates are given by  $d_1$ ,  $d_2$ ,  $d_3$ , and  $d_4$ , whereas recovery rates are denoted by  $\gamma_1$  through  $\gamma_5$ .

Our findings suggest that some exposed individuals are capable of transmitting the virus, and infected patients may experience varying degrees of symptom severity. Accordingly, we assume that infectious patients treated in regular hospitals can progress to more severe stages at rates  $h_1$ ,  $h_2$ , and  $h_3$ . Similarly, ICU patients without oxygen support may deteriorate at rates  $\lambda_1$  and  $\lambda_2$ , while those receiving oxygen in the ICU may advance to critical condition at rate  $\epsilon$ .

The model also incorporates prevention and treatment interventions. Specifically,  $\phi_1$  represents the vaccination rate of susceptible individuals, while  $\phi_2$  corresponds to control measures for exposed individuals, including quarantine, social distancing, mask usage, and basic healthcare provision. The parameters  $\phi_3$ ,  $\phi_4$ , and  $\phi_5$  denote treatment rates for infected patients in field hospitals, ICU without oxygen, and ICU with oxygen support, respectively.

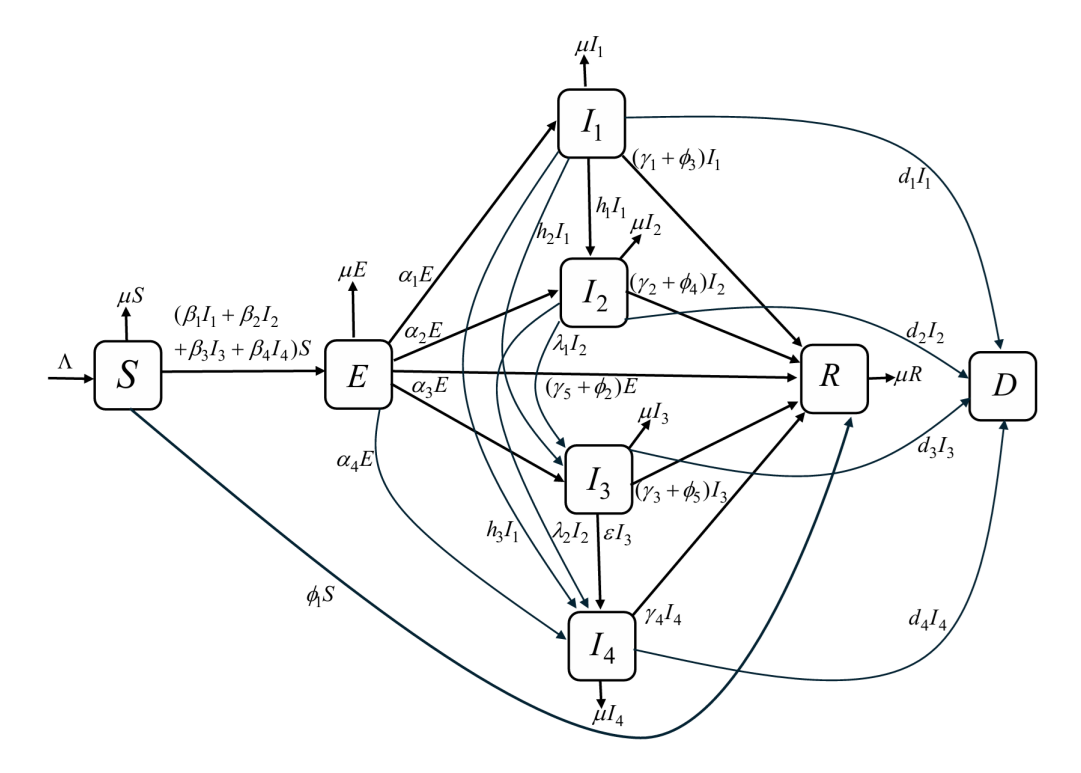


Figure 1: Diagram on the dynamical transmission of COVID-19.

As a result, we obtain the following dynamical system (see Figure 1 for its diagram):

$$\frac{dS}{dt} = \Lambda - (\beta_1 I_1 + \beta_2 I_2 + \beta_3 I_3 + \beta_4 E) S - (\mu + \phi_1) S, \tag{2.1}$$

$$\frac{dE}{dt} = (\beta_1 I_1 + \beta_2 I_2 + \beta_3 I_3 + \beta_4 E) S - (\alpha_1 + \alpha_2 + \alpha_3 + \alpha_4 + \mu + \gamma_5 + \phi_2) E, \tag{2.2}$$

$$\frac{dI_1}{dt} = \alpha_1 E - (\mu + d_1 + \gamma_1 + h_1 + h_2 + h_3 + \phi_3)I_1, \tag{2.3}$$

$$\frac{dI_{2}}{dt} = \alpha_{2}E + h_{1}I_{1} - (\mu + d_{2} + \gamma_{2} + \lambda_{1} + \lambda_{2} + \phi_{4})I_{2}, \tag{2.4}$$

$$\frac{dI_{3}}{dt} = \alpha_{3}E + h_{2}I_{1} + \lambda_{1}I_{2} - (\mu + d_{3} + \gamma_{3} + \varepsilon + \phi_{5})I_{3}, \tag{2.5}$$

$$\frac{dI_4}{dt} = \alpha_4 E + h_3 I_1 + \lambda_2 I_2 + \varepsilon I_3 - (\mu + d_4 + \gamma_4) I_4, \tag{2.6}$$

$$\frac{dR}{dt} = \phi_1 S + (\gamma_1 + \phi_3) I_1 + (\gamma_2 + \phi_4) I_2 + (\gamma_3 + \phi_5) I_3 + \gamma_4 I_4 + (\gamma_5 + \phi_2) E - \mu R, \tag{2.7}$$

$$\frac{dD}{dt} = d_1 I_1 + d_2 I_2 + d_3 I_3 + d_4 I_4, \tag{2.8}$$

with the initial conditions  $S(0) \ge 0$ ,  $E(0) \ge 0$ ,  $I_1(0) \ge 0$ ,  $I_2(0) \ge 0$ ,  $I_3(0) \ge 0$ ,  $I_4(0) \ge 0$ ,  $R(0) \ge 0$ , and  $D(0) \ge 0$ . First, we determine the boundary of the system of equations (2.1)-(2.8). Consider,

$$\begin{split} \frac{dN}{dt} &= \frac{dS}{dt} + \frac{dE}{dt} + \frac{dI_1}{dt} + \frac{dI_2}{dt} + \frac{dI_3}{dt} + \frac{dI_4}{dt} + \frac{dR}{dt} + \frac{dD}{dt} \\ &= \Lambda - \left(\beta_1 I_1 + \beta_2 I_2 + \beta_3 I_3 + \beta_4 E\right) S - (\mu + \varphi_1) S + \left(\beta_1 I_1 + \beta_2 I_2 + \beta_3 I_3 + \beta_4 E\right) S \\ &- (\alpha_1 + \alpha_2 + \alpha_3 + \alpha_4 + \mu + \gamma_5 + \varphi_2) E + \alpha_1 E - (\mu + d_1 + \gamma_1 + h_1 + h_2 + h_3 + \varphi_3) I_1 \\ &+ \alpha_2 E + h_1 I_1 - (\mu + d_2 + \gamma_2 + \lambda_1 + \lambda_2 + \varphi_4) I_2 + \alpha_3 E + h_2 I_1 + \lambda_1 I_2 - (\mu + d_3 + \gamma_3 + \epsilon + \varphi_5) I_3 \\ &+ \alpha_4 E + h_3 I_1 + \lambda_2 I_2 + \epsilon I_3 - (\mu + d_4 + \gamma_4) I_4 + \varphi_1 S + (\gamma_1 + \varphi_3) I_1 + (\gamma_2 + \varphi_4) I_2 + (\gamma_3 + \varphi_5) I_3 + \gamma_4 I_4 \\ &+ (\gamma_5 + \varphi_2) E - \mu R + d_1 I_1 + d_2 I_2 + d_3 I_3 + d_4 I_4 \\ &= \Lambda + \mu D - \mu (S + E + I_1 + I_2 + I_3 + I_4 + R + D) = \Lambda + \mu D - \mu N. \end{split}$$

It gives that

$$\limsup_{t\to\infty} N(t) \leqslant \frac{\Lambda}{\mu} + \mu M.$$

Thus, the considered region for this model is

$$\Omega = \left\{ \left(S, E, I_1, I_2, I_3, I_4, R, D\right) \in \mathbb{R}_+^8 : 0 \leqslant S + E + I_1 + I_2 + I_3 + I_4 + R + D \leqslant \frac{\Lambda}{\mu} + \mu M \right. \right\}.$$

All solutions of this model are bounded and enter the region  $\Omega$  and M is the total number of death individuals due to COVID-19 infections. Hence,  $\Omega$  is a positively invariant. That is every solution of this model remains there for all t>0.

The next section presents an equilibrium analysis to establish the existence of equilibrium points.

#### 3. Equilibrium analysis

Next we find the disease free equilibrium point(DFE) by setting E,  $I_1$ ,  $I_2$ ,  $I_3$ ,  $I_4$ , and D in the equations equal to zero and solve for S and R. Thus from equation (2.1), we have

$$S = \frac{\Lambda}{\mu + \phi_1}$$

and from equation (2.7), we have

$$R = \frac{\varphi_1 \Lambda}{\mu(\mu + \varphi_1)}.$$

Therefore, the DFE for the system is denoted by

$$\varepsilon_0 = \Big(\frac{\Lambda}{\mu + \varphi_1}, 0, 0, 0, 0, 0, \frac{\varphi_1 \Lambda}{\mu(\mu + \varphi_1)}, 0\Big).$$

The following subsection derives the reproduction number of the model.

# 3.1. Basic reproduction number $(R_0)$

Next, we will find the basic reproduction number by using the next-generation method [41] (for all details, please see Appendix B):

$$R_{0} = \frac{\Lambda\left(\beta_{4}\,\ell_{2}\,\ell_{3}\,\ell_{4} + \alpha_{1}\beta_{1}\,\ell_{3}\,\ell_{4} + \beta_{2}\left(\alpha_{1}h_{1} + \alpha_{2}\ell_{2}\right)\ell_{4} + \beta_{3}\left(\alpha_{3}\ell_{2}\ell_{3} + \alpha_{1}h_{2}\ell_{3} + \alpha_{1}h_{1}\lambda_{1} + \alpha_{2}\lambda_{1}\ell_{2}\right)\right)}{\left(\mu + \varphi_{1}\right)\ell_{1}\,\ell_{2}\,\ell_{3}\,\ell_{4}},$$

where

$$\begin{split} \ell_1 &= \alpha_1 + \alpha_2 + \alpha_3 + \alpha_4 + \mu + \gamma_5 + \varphi_2, \\ \ell_3 &= \mu + d_2 + \gamma_2 + \lambda_1 + \lambda_2 + \varphi_4, \end{split} \qquad \begin{aligned} \ell_2 &= \mu + d_1 + \gamma_1 + h_1 + h_2 + h_3 + \varphi_3, \\ \ell_4 &= \mu + d_3 + \gamma_3 + \epsilon + \varphi_5. \end{aligned}$$

Consequently, based on the work in the paper proposed by Van Den Driessche and Watmough[41], we immediately have the following result.

**Theorem 3.1.** The disease-free equilibrium of the model is locally asymptotically stable if  $R_0 < 1$ , and unstable if  $R_0 > 1$ .

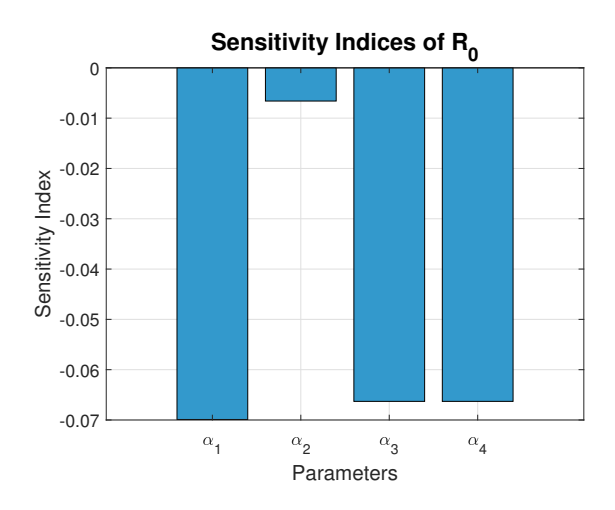
In the next section, we use sensitivity analysis to identify the parameters that most strongly influence the increase in the reproduction number.

# 4. Sensitivity analysis

In this section, we will conduct a sensitivity analysis of  $R_0$  with respect to the parameters, which will be evaluated using the baseline parameter values provided in Table 2. We use the normalized forward sensitivity index for this purpose, specifically focusing on  $R_0$ , which depends on the differentiability of a parameter  $\eta$ . The normalized forward sensitivity index is defined as  $\Upsilon_{\eta}^{R_0} = \frac{\partial R_0}{\partial \eta} \times \frac{\eta}{R_0}$  (refer to [7]). Table 1 presents the sensitivity indices of  $R_0$  concerning each parameter.

As depicted in Table 1,  $\beta_1$ ,  $\beta_2$ ,  $\beta_3$ ,  $\beta_4$ , and  $\Lambda$  have a positive sensitivity index, indicating that an increase in these parameters leads to an increase in the value of  $R_0$ . Conversely,  $\alpha_1$ ,  $\alpha_2$ ,  $\alpha_3$ ,  $\alpha_4$ ,  $h_1$ ,  $h_2$ ,  $d_1$ ,  $d_2$ ,  $d_3$ ,  $h_3$ ,  $\mu$ ,  $\epsilon$ ,  $\gamma_1$ ,  $\gamma_2$ ,  $\gamma_3$ ,  $\gamma_5$ ,  $\phi_1$ ,  $\phi_2$ ,  $\phi_3$ ,  $\phi_4$ ,  $\phi_5$ ,  $\lambda_1$ , and  $\lambda_2$  exhibit a negative sensitivity index, indicating that an increase in their values leads to a decrease in the basic reproduction number. We can observe that the vaccination rate,  $\phi_1$ , exhibits the most negative sensitivity. Specifically,  $\Upsilon_{\phi_1}^{R_0} = -0.9223$ , indicating that a 10% increase in the parameter  $\phi_1$  results in a 9.223% reduction in the value of  $R_0$ 

To effectively reduce the outbreak, emphasis should be placed on optimal control strategies involving vaccination ( $\phi_1$ ), treatment rates for infected individuals in field hospitals ( $\phi_2$ ), regular hospitals ( $\phi_3$ ), ICUs without oxygen tubes ( $\phi_4$ ), and ICUs with oxygen tubes ( $\phi_5$ ). In particular,  $\phi_1$  for susceptible individuals and  $\phi_2$  for exposed and infectious individuals play a key role in lowering infection rates. Since the sensitivity indices of most parameters are relatively small, we present bar plots only for  $\alpha_1$ ,  $\alpha_2$ ,  $\alpha_3$ ,  $\alpha_4$  and  $\beta_1$ ,  $\beta_2$ ,  $\beta_3$ ,  $\beta_4$ , as shown in Figures 2 and 3, respectively. The analysis shows that  $\beta_4$  and  $\Lambda$  have the largest positive impact; however, since  $\Lambda$  represents the recruitment rate, our focus will be on reducing infections by targeting the transmission rates  $\beta_1$ ,  $\beta_2$ ,  $\beta_3$ ,  $\beta_4$  instead.



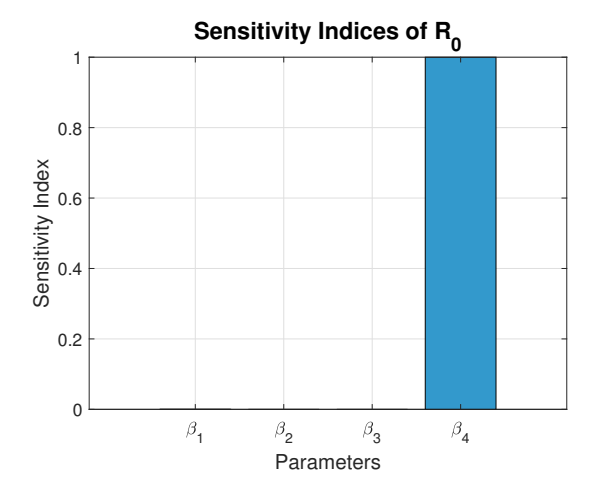


Figure 2: Sensitivity indices of parameters in the basic reproduction number

Figure 3: Sensitivity indices of parameters in the basic reproduction number. The values of  $\beta_1$ ,  $\beta_2$ , and  $\beta_3$  are extremely small-close to zero-and therefore do not appear in the graph.

Table 1: Numerical values of sensitivity indices of R<sub>0</sub>.

Parameter	Sensitivity index	Parameter	Sensitivity index
$\alpha_1$	-0.0699	μ	-0.0780
$\alpha_2$	-0.0066	Λ	+1.0000
$\alpha_3$	-0.0663	$\epsilon$	$-5.6213 \times 10^{-12}$
$lpha_4$	-0.0663	$\gamma_1$	$-4.4112 \times 10^{-6}$
$d_1$	$-3.0843 \times 10^{-9}$	$\gamma_2$	$-1.9572 \times 10^{-7}$
$d_2$	$-1.3980 \times 10^{-9}$	$\gamma_3$	$-4.6825 \times 10^{-8}$
$d_3$	$-5.7017 \times 10^{-10}$	$\gamma_5$	-0.1004
$h_1$	$-1.2991 \times 10^{-8}$	$\phi_1$	-0.9223
$h_2$	$-8.1810 \times 10^{-10}$	$\Phi_2$	-0.6902
$h_3$	$-8.1920 \times 10^{-12}$	$\phi_3$	$-3.2768 \times 10^{-5}$
$eta_1$	$+3.7200 \times 10^{-5}$	$\phi_4$	$-9.7859 \times 10^{-12}$
$\beta_2$	$+1.9822 \times 10^{-7}$	$\Phi_5$	$-5.6213 \times 10^{-12}$
$\beta_3$	$+4.7431 \times 10^{-8}$	$\lambda_1$	$-9.5510 \times 10^{-10}$
$oxed{\beta_4}$	+1	$\lambda_2$	$-9.7859 \times 10^{-11}$

In the next section, we verify the existence of an equilibrium point and examine its stability.

# 5. Global stability of the disease-free equilibrium

Next, we examine the global asymptotic stability of the DFE. To that end we state the following result introduced by Castillo-Chavez et al. [6].

Lemma 5.1. Consider a model system written in the form

$$\frac{dX_1}{dt} = F(X_1, X_2), \quad \frac{dX_2}{dt} = G(X_1, X_2), \quad G(X_1, 0) = 0,$$

where  $X_1 \in \mathbb{R}^m$  denotes (its components) the number of uninfected individuals and  $X_2 \in \mathbb{R}^n$  denotes (its components) the number of infected individuals including latent, infectious, etc;  $X_0 = (X_1^*)$  denotes the disease-free equilibrium of the system. Also assume the following conditions.

(H1) For  $\frac{dX_1}{dt} = F(X_1^*, 0)$ ,  $X_1^*$  is globally asymptotically stable.

(H2)  $G(X_1, X_2) = AX_2 - \hat{G}(X_1, X_2), \ \hat{G}(X_1, X_2) \geqslant 0 \ \text{for} \ (X_1, X_2) \in \Omega, \ \text{where the Jacobian} \ A = \frac{\partial G}{\partial X_2}(X_1^*, 0) \ \text{is}$ an M-matrix (the off diagonal elements of A are non-negative) and  $\Omega$  is the region where the model makes biological sense.

Then the DFE  $X_0 = (X_1^*, 0)$  is globally asymptotically stable provided that  $R_0 < 1$ .

**Theorem 5.2.** The disease-free equilibrium of the model is globally asymptotic stable when  $R_0 < 1$ .

Proof. We adopt the notations in Lemma 5.1, and verify the conditions (H1) and (H2). In our ODE system,  $X_1 = (S, R), X_2 = (E, I_1, I_2, I_3, I_4, D)$  and  $X_1^* = \left(\frac{\Lambda}{\mu + \varphi_1}, \frac{\varphi_1 \Lambda}{\mu(\mu + \varphi_1)}\right)$ . Now when  $X_2 = 0$ , we have

$$\frac{dX_1}{dt} = \left[ \begin{array}{c} \Lambda - (\mu + \phi_1)S \\ \phi_1 S - \mu R \end{array} \right].$$

As for S, we have from the above that  $\frac{dS}{dt} = \Lambda - (\mu + \varphi_1)S$ , and thus it gives  $S(t) = \frac{\Lambda}{\mu + \varphi_1} + C_1 e^{-(\mu + \varphi_1)t}$  for arbitrary constant value of  $C_1$ . Similarly with the equation  $\frac{dR}{dt} + \mu R = \varphi_1 S$ , by using the same technique, we then have  $R(t) = \frac{\varphi_1 \Lambda}{\mu(\mu + \varphi_1)} + C_2 e^{-\mu t}$  for arbitrary constant value of  $C_2$ . Clearly,  $S(t) \to \frac{\Lambda}{\mu + \varphi_1}$  and  $R(t) \to \frac{\varphi_1 \Lambda}{\mu(\mu + \varphi_1)}$ , as  $t \to \infty$ . Thus  $X_1^* = \left(\frac{\Lambda}{\mu + \varphi_1}, \frac{\varphi_1 \Lambda}{\mu(\mu + \varphi_1)}\right)$  is globally asymptotically stable. Next consider

$$\frac{dX_2}{dt} = \begin{bmatrix} \left(\beta_1 I_1 + \beta_2 I_2 + \beta_3 I_3 + \beta_4 E\right) S - e_1 E \\ \alpha_1 E - e_2 I_1 \\ \alpha_2 E + h_1 I_1 - e_3 I_2 \\ \alpha_3 E + h_2 I_1 + \lambda_1 I_2 - e_4 I_3 \\ \alpha_4 E + h_3 I_1 + \lambda_2 I_2 + \epsilon I_3 - e_5 I_4 \\ d_1 I_1 + d_2 I_2 + d_3 I_3 + d_4 I_4 \end{bmatrix},$$

 $\text{where } e_1 = \alpha_1 + \alpha_2 + \alpha_3 + \alpha_4 + \mu + \gamma_5 + \varphi_2 \text{, } e_2 = \mu + d_1 + \gamma_1 + h_1 + h_2 + h_3 + \varphi_3 \text{, } e_3 = \mu + d_2 + \gamma_2 + \lambda_1 + d_3 + d_4 + \mu + \gamma_5 + \varphi_4 \text{, } e_4 = \mu + d_1 + \gamma_1 + h_2 + h_3 + \varphi_4 \text{, } e_5 = \mu + d_2 + \gamma_2 + \lambda_1 + d_3 + \varphi_4 \text{, } e_5 = \mu + d_2 + \gamma_2 + \lambda_1 + d_3 + \varphi_5 \text{, } e_5 = \mu + d_2 + \gamma_2 + \lambda_1 + d_3 + \varphi_5 \text{, } e_5 = \mu + d_2 + \gamma_2 + \lambda_1 + d_3 + \varphi_5 \text{, } e_5 = \mu + d_2 + \varphi_5 + \varphi_5 \text{, } e_5 = \mu + d_3 + \varphi_5 \text{, } e_5 = \mu +$  $\lambda_2 + \phi_4$ ,  $e_4 = \mu + d_3 + \gamma_3 + \varepsilon + \phi_5$ ,  $e_5 = \mu + d_4 + \gamma_4$ , and at the equilibrium point of the subsystem  $X_1$ , we have

$$\frac{\partial G}{\partial X_2} = \left[ \begin{array}{cccccc} -e_1 + \beta_4 S & \beta_1 S & \beta_2 S & \beta_3 S & 0 & 0 \\ \alpha_1 & -e_2 & 0 & 0 & 0 & 0 \\ \alpha_2 & h_1 & -e_3 & 0 & 0 & 0 \\ \alpha_3 & h_2 & \lambda_1 & -e_4 & 0 & 0 \\ \alpha_4 & h_3 & \lambda_2 & \epsilon & -e_5 & 0 \\ 0 & d_1 & d_2 & d_3 & d_4 & 0 \end{array} \right].$$

Now, by the Lemma 5.1,

$$\frac{\partial G}{\partial X_2}(X_1^*,0) = \begin{bmatrix} -e_1 + \frac{\beta_4 \Lambda}{\mu + \phi_1} & \frac{\beta_1 \Lambda}{\mu + \phi_1} & \frac{\beta_2 \Lambda}{\mu + \phi_1} & \frac{\beta_3 \Lambda}{\mu + \phi_1} & 0 & 0 \\ \alpha_1 & -e_2 & 0 & 0 & 0 & 0 \\ \alpha_2 & h_1 & -e_3 & 0 & 0 & 0 \\ \alpha_3 & h_2 & \lambda_1 & -e_4 & 0 & 0 \\ \alpha_4 & h_3 & \lambda_2 & \varepsilon & -e_5 & 0 \\ 0 & d_1 & d_2 & d_3 & d_4 & 0 \end{bmatrix}.$$

Now from (H2), we need to show that  $\hat{G}(X_1, X_2)$  satisfies the equation

$$G(X_1, X_2) = AX_2 - \hat{G}(X_1, X_2)$$

and  $\hat{G}(X_1, X_2)$  has to be greater than or equal to zero. Note that

$$\hat{G}(X_1, X_2) = AX_2 - G(X_1, X_2),$$

$$= \begin{bmatrix} -e_1 + \frac{\beta_4 \Lambda}{\mu + \varphi_1} & \frac{\beta_1 \Lambda}{\mu + \varphi_1} & \frac{\beta_2 \Lambda}{\mu + \varphi_1} & \frac{\beta_3 \Lambda}{\mu + \varphi_1} & 0 & 0 \\ \alpha_1 & -e_2 & 0 & 0 & 0 & 0 \\ \alpha_2 & h_1 & -e_3 & 0 & 0 & 0 \\ \alpha_3 & h_2 & \lambda_1 & -e_4 & 0 & 0 \\ \alpha_4 & h_3 & \lambda_2 & \epsilon & -e_5 & 0 \\ 0 & d_1 & d_2 & d_3 & d_4 & 0 \end{bmatrix} \begin{bmatrix} E \\ I_1 \\ I_2 \\ I_3 \\ I_4 \\ D \end{bmatrix}$$
 
$$- \begin{bmatrix} \left(\beta_1 I_1 + \beta_2 I_2 + \beta_3 I_3 + \beta_4 E\right) S - e_1 E \\ \alpha_1 E - e_2 I_1 \\ \alpha_2 E + h_1 I_1 - e_3 I_2 \\ \alpha_3 E + h_2 I_1 + \lambda_1 I_2 - e_4 I_3 \\ \alpha_4 E + h_3 I_1 + \lambda_2 I_2 + \epsilon I_3 - e_5 I_4 \\ d_1 I_1 + d_2 I_2 + d_3 I_3 + d_4 I_4 \end{bmatrix} = \begin{bmatrix} \left(\beta_1 I_1 + \beta_2 I_2 + \beta_3 I_3 + \beta_4 E\right) \left(\frac{\Lambda}{\mu + \varphi_1} - S\right) \\ 0 \\ 0 \\ 0 \\ 0 \end{bmatrix},$$

given that  $S\leqslant \frac{\Lambda}{\mu+\varphi_1}$ , where  $X_1$  and  $X_2$  are in  $\Omega$ . Hence it is clearly seen that  $\hat{G}(X_1,X_2)\geqslant 0$ . Therefore, by Lemma 5.1 the DFE  $X_0=(X_1^*,0)$  is globally asymptotically stable.

## 6. The endemic equilibrium point and stability analysis

We first investigate the existence of the positive endemic equilibrium point, denoted by  $\epsilon^* = (S^*, E^*, I_1^*, I_2^*, I_3^*, I_4^*, R^*)$ . This endemic equilibrium is determined by the following equations:

$$0 = \Lambda - \left(\beta_1 I_1^* + \beta_2 I_2^* + \beta_3 I_3^* + \beta_4 E^*\right) S^* - (\mu + \phi_1) S^*, \tag{6.1}$$

$$0 = (\beta_1 I_1^* + \beta_2 I_2^* + \beta_3 I_3^* + \beta_4 E^*) S^* - (\alpha_1 + \alpha_2 + \alpha_3 + \alpha_4 + \mu + \gamma_5 + \phi_2) E^*,$$
(6.2)

$$0 = \alpha_1 E^* - (\mu + d_1 + \gamma_1 + h_1 + h_2 + h_3 + \phi_3) I_1^*, \tag{6.3}$$

$$0 = \alpha_2 E^* + h_1 I_1^* - (\mu + d_2 + \gamma_2 + \lambda_1 + \lambda_2 + \phi_4) I_2^*, \tag{6.4}$$

$$0 = \alpha_3 E^* + h_2 I_1^* + \lambda_1 I_2^* - (\mu + d_3 + \gamma_3 + \varepsilon + \phi_5) I_3^*, \tag{6.5}$$

$$0 = \alpha_4 E^* + h_3 I_1^* + \lambda_2 I_2^* + \varepsilon I_3^* - (\mu + d_4 + \gamma_4) I_4^*, \tag{6.6}$$

$$0 = \phi_1 S^* + (\gamma_1 + \phi_3) I_1^* + (\gamma_2 + \phi_4) I_2^* + (\gamma_3 + \phi_5) I_3^* + \gamma_4 I_4^* + (\gamma_5 + \phi_2) E^* - \mu R^*. \tag{6.7}$$

From equations (6.3) and (6.4), we obtain

$$I_1^* = \frac{\alpha_1 E^*}{l_2},\tag{6.8}$$

and

$$I_2^* = \frac{(\alpha_2 l_2 + h_1 \alpha_1) E^*}{l_2 l_3},$$
(6.9)

respectively. Next we consider equations (6.5) and (6.6), we get

$$I_3^* = \frac{(\alpha_3 l_2 l_3 + \alpha_1 h_2 l_3 + \lambda_1 (\alpha_2 l_2 + h_1 \alpha_1)) E^*}{l_2 l_3 l_4}$$
(6.10)

and

$$I_4^* = \frac{(\alpha_4 l_2 l_3 l_4 + \alpha_1 h_3 l_3 l_4 + \lambda_2 (\alpha_2 l_2 + \alpha_1 h_1) l_4 + (\alpha_3 l_2 l_3 + \alpha_1 h_2 l_3 + \lambda_1 (\alpha_2 l_2 + h_1 \alpha_1)))E^*}{l_2 l_3 l_4 l_5},$$

respectively. Substituting  $I_1^*$ ,  $I_2^*$ ,  $I_3^*$ , and  $I_4^*$  into equation (6.7), we obtain

$$R^* = \frac{1}{\mu l_2 l_3 l_4 l_5} \Bigg[ ((\gamma_1 + \varphi_3)\alpha_1 l_3 l_4 l_5 + (\gamma_2 + \varphi_4)(\alpha_2 l_2 + \alpha_1 h_1) l_4 l_5 + (\gamma_3 + \varphi_5)(\alpha_3 l_2 l_3 + (\gamma_3 + \varphi_5)(\alpha_3 l_2 l_3 + (\gamma_3 + \varphi_5)(\alpha_3 l_3 l_4 l_5 + (\gamma_3 + \varphi_5)(\alpha_3 l_4 l_5 + (\gamma_5 + \varphi_5)(\alpha_3 l_4 l_5 + (\gamma_5 + \varphi_5)(\alpha_5 l_4 l_5 + (\gamma_5 + \varphi_5)(\alpha_5 l_4 l_5 + (\gamma_5 + \varphi_5)(\alpha_5 l_5$$

$$\left. + \alpha_1 h_2 l_3 + \lambda_1 (\alpha_2 l_2 + h_1 \alpha_1)) l_5 + \gamma_4 (\alpha_4 l_2 l_3 l_4 + \alpha_1 h_3 l_3 l_4 + \lambda_2 (\alpha_2 l_2 + \alpha_1 h_1) l_4 \right. \\ \left. + (\alpha_3 l_2 l_3 + \alpha_1 h_2 l_3 + \lambda_1 (\alpha_2 l_2 + h_1 \alpha_1)) + (\gamma_5 + \varphi_5) l_2 l_3 l_4 l_5)) E^* + \varphi_1 l_2 l_3 l_4 l_5 S^* \right].$$

From (6.8), (6.9), and (6.10), we have

$$I_1^* = M_1 E^*, \quad I_2^* = M_2 E^*, \quad I_3^* = M_3 E^*,$$
 (6.11)

with  $M_1 = \frac{\alpha_1}{l_2}$ ,  $M_2 = \frac{(\alpha_2 l_2 + h_1 \alpha_1)}{l_2 l_3}$ , and  $M_3 = \frac{(\alpha_3 l_2 l_3 + \alpha_1 h_2 l_3 + \lambda_1 (\alpha_2 l_2 + h_1 \alpha_1))}{l_2 l_3 l_4}$ . For  $E^* \neq 0$ , substituting equations (6.11) into equation (6.1), we obtain that  $S^* = \frac{\Lambda}{(\beta_1 M_1 + \beta_2 M_2 + \beta_3 M_3 + \beta_4) E^* + \mu + \varphi_1}.$  (6.12)

$$S^* = \frac{\Lambda}{(\beta_1 M_1 + \beta_2 M_2 + \beta_3 M_3 + \beta_4) E^* + \mu + \phi_1}.$$
 (6.12)

Furthermore, substituting equations (6.11) into equation (6.2), we have

$$S^* = \frac{l_1}{\beta_1 M_1 + \beta_2 M_2 + \beta_3 M_3 + \beta_4}. (6.13)$$

Substituting (6.12) into (6.13) for  $E = E^*$ , we get  $g_1(E) = g_2(E)$ , where

$$g_1(E) = \frac{\Lambda}{(\beta_1 M_1 + \beta_2 M_2 + \beta_3 M_3 + \beta_4)E + \mu + \varphi_1}, \quad g_2(E) = \frac{l_1}{\beta_1 M_1 + \beta_2 M_2 + \beta_3 M_3 + \beta_4}.$$

Clearly, both  $g_1$  and  $g_2$  are differentiable functions for  $E \ge 0$ . Taking the derivative of  $g_1$  and  $g_2$  yields the following:

$$g_2'(\mathsf{E}) = 0, \quad g_1'(\mathsf{E}) = \frac{-\Lambda(\beta_1 M_1 + \beta_2 M_2 + \beta_3 M_3 + \beta_4)}{((\beta_1 M_1 + \beta_2 M_2 + \beta_3 M_3 + \beta_4)\mathsf{E} + \mu + \phi_1)^2} < 0.$$

Therefore, on the interval  $[0,\infty]$ ,  $g_1(E)$  is a decreasing function while  $g_2(E)$  remains constant. We can easily observe that if  $R_0 > 1$ , then  $g_1(0) > g_2(0)$ , which implies that there is a unique endemic equilibrium at  $E = E^*$ . However, if  $R_0 \le 1$ , then  $g_1(0) > g_2(0)$ , and there is no endemic equilibrium. This result is summarized below.

**Theorem 6.1.** When  $R_0 > 1$ , there exists a unique endemic equilibrium of the system (2.1)-(2.7).

# 6.1. Local stability of the endemic equilibrium point

**Theorem 6.2.** The endemic equilibrium point  $(\varepsilon^*)$  is stable if it satisfies the Routh-Hurwitz criteria, where  $I_i^* \geqslant 1$ when i = 1, 2, 3.

*Proof.* One can reduce the system (2.1)-(2.7) to a six-dimensional system by setting  $R = N - S - E - I_1 - I_2$  $I_2 - I_3 - I_4$ , we exclude D here since it does not affects other states, resulting in the Jacobian matrix of the endemic equilibrium point,  $\epsilon^*$ , being

$$J(\epsilon^*) = \begin{bmatrix} -(A_1 + \mu + \phi) & -\beta_4 S^* & -\beta_1 & -\beta_2 & -\beta_3 & 0 \\ A_1 & \beta_4 S^* - l_1 & \beta_1 & \beta_2 & \beta_3 & 0 \\ 0 & \alpha_1 & -l_2 & 0 & 0 & 0 \\ 0 & \alpha_2 & h_1 & -l_3 & 0 & 0 \\ 0 & \alpha_3 & h_2 & \lambda_1 & -l_4 & 0 \\ 0 & \alpha_4 & h_3 & \lambda_2 & \epsilon & -l_5 \end{bmatrix},$$

 $\text{where } A_1 = \beta_1 I_1^* + \beta_2 I_2^* + \beta_3 I_3^* + \beta_4 E^*. \text{ The eigenvalues of } J(\varepsilon^*) \text{ are calculated using } \det(J(\varepsilon^*) - \lambda I) = 0,$ and we obtain that

$$(-l_5-\lambda)(\lambda^5+\alpha_1\lambda^4+\alpha_2\lambda^3+\alpha_3\lambda^2+\alpha_4\lambda+\alpha_5)=0\text{,}$$

where

$$\begin{split} & \mathfrak{a}_1 = l_1 + l_2 + l_3 + A_1 + \mu + \varphi_1 - \beta_4 S^*, \\ & \mathfrak{a}_2 = l_3 l_4 + l_1 l_3 + l_2 l_3 + + l_1 l_2 + l_1 l_4 + A_1 l_3 + A_1 l_1 + A_1 l_2 + (\mu + \varphi_1) (l_1 + l_2 + l_3 - \beta_4 S^*) - \beta_3 \alpha_3 \\ & - \beta_4 S^* l_4 - \beta_2 \alpha_2 - \beta_4 S^* l_3 - \beta_4 S^* l_2 - \alpha_1 \beta_1, \\ & \mathfrak{a}_3 = l_1 l_2 l_3 + l_1 l_3 l_4 + l_2 l_3 l_4 + l_1 l_2 l_4 + A_1 l_3 l_4 + A_1 l_1 l_3 + A_1 l_2 l_3 + A_1 l_1 l_2 + A_1 l_1 l_4 - \beta_3 \alpha_3 l_3 - \beta_3 \alpha_1 h_2 \\ & - \beta_3 \alpha_3 l_2 - \beta_3 \alpha_2 \lambda_1 - \beta_2 \alpha_2 l_4 - \beta_4 S^* l_3 l_4 - \beta_4 S^* l_2 l_3 - \alpha_1 \beta_1 l_4 - \beta_2 \alpha_1 h_1 - \beta_2 \alpha_2 l_2 - \beta_4 S^* l_2 l_3 \\ & - \beta_1 \alpha_1 l_3 + (l_1 l_4 + l_1 l_3 + l_2 l_3 + l_1 l_2 - \beta_3 \alpha_3 - \beta_4 S^* l_4 - \beta_2 \alpha_2 - \beta_4 S^* l_3 - \beta_4 S^* l_2 - \alpha_1 \beta_1) (\mu + \varphi_1), \\ & \mathfrak{a}_4 = l_1 l_2 l_3 l_4 + A_1 l_1 l_3 l_4 + A_1 l_1 l_2 l_4 + A_1 l_1 l_2 l_3 - \beta_3 \alpha_1 h_2 l_3 - \beta_3 \alpha_3 l_2 l_3 - \beta_3 \alpha_1 h_1 \lambda_1 - \beta_3 \alpha_2 l_2 \lambda_1 \\ & - \beta_2 \alpha_1 h_1 l_4 - \beta_2 \alpha_2 l_2 l_4 - \beta_4 S^* l_2 l_3 l_4 - \alpha_1 \beta_1 l_3 l_4 + (\mu + \varphi_1) (l_1 l_3 l_4 + l_2 l_3 l_4 + l_1 l_2 l_4 + l_1 l_2 l_3 - \beta_3 \alpha_3 l_3 \\ & - \beta_3 \alpha_1 h_2 - \beta_3 \alpha_3 l_2 - \beta_3 \alpha_2 \lambda_1 - \beta_2 \alpha_2 l_4 - \beta_4 S^* l_3 l_4 - \beta_4 S^* l_2 l_3 - \alpha_1 \beta_1 l_4 \\ & - \beta_2 \alpha_1 h_1 - \beta_2 \alpha_2 l_2 - \beta_4 S^* l_2 l_4 - \alpha_1 \beta_1 l_3), \\ & \mathfrak{a}_5 = A_1 l_1 l_2 l_3 l_4 + (l_1 l_2 l_3 l_4 - \beta_3 \alpha_1 h_2 l_3 - \beta_3 \alpha_3 l_2 l_3 - \beta_3 \alpha_1 h_1 \lambda_1 - \beta_3 \alpha_2 l_2 \lambda_1 \\ & - \beta_2 \alpha_1 h_1 l_4 - \beta_2 \alpha_2 l_2 l_4 - \beta_4 S^* l_2 l_3 l_4 - \beta_1 \alpha_1 l_3 l_4) (\mu + \varphi_1). \end{aligned}$$

Therefore, the first eigenvalue is  $-l_5$ , which is negative. Next, we consider the polynomial equation  $\lambda^5 + a_1\lambda^4 + a_2\lambda^3 + a_3\lambda^2 + a_4\lambda + a_5 = 0$ . According to the Routh-Hurwitz criterion, the endemic equilibrium point is locally asymptotically stable if:

- (i)  $a_i > 0$ , i = 1, 2, 3, 4, 5;
- (ii)  $a_1 a_2 a_3 > a_3^2 + a_1^2 a_4$ ; and
- (iii)  $(a_1a_4 a_5)(a_1a_2a_3 a_3^2 a_1^2a_4) > a_5(a_1a_2 a_3)^2 + a_1a_5^2$

For details on all criteria, please refer to Appendix A.

## 6.2. Global stability of the endemic equilibrium

In this section, we will also establish the global stability of the endemic equilibrium of system (2.1)-(2.7) by using a Lyapunov function.

**Theorem 6.3.** The unique endemic equilibrium point  $(\varepsilon^*)$  of system (2.1)-(2.7) is globally asymptotically stable when  $R_0 > 1$ .

*Proof.* The system represented by equations (2.1)-(2.5) can be transformed into the following form:

$$\begin{split} \frac{dS}{dt} &= S \left( \frac{\Lambda}{S^*} \left( \frac{S^*}{S} - 1 \right) - \beta_1 I_1^* \left( \frac{I_1}{I_1^*} - 1 \right) - \beta_2 I_2^* \left( \frac{I_2}{I_2^*} - 1 \right) - \beta_3 I_3^* \left( \frac{I_3}{I_3^*} - 1 \right) - \beta_4 E^* \left( \frac{E}{E^*} - 1 \right) \right), \\ \frac{dE}{dt} &= \frac{\beta_1 I_1^* S^* E}{E^*} \left( \frac{I_1 S E^*}{I_1^* S^* E} - 1 \right) + \frac{\beta_2 I_2^* S^* E}{E^*} \left( \frac{I_2 S E^*}{I_2^* S^* E} - 1 \right) \frac{\beta_3 I_3^* S^* E}{E^*} \left( \frac{I_3 S E^*}{I_3^* S^* E} - 1 \right) + \beta_4 E S^* \left( \frac{S}{S^*} - 1 \right), \\ \frac{dI_1}{dt} &= \frac{\alpha_1 E^* I_1}{I_1^*} \left( \frac{E I_1^*}{E^* I_1} - 1 \right), \\ \frac{dI_2}{dt} &= \frac{\alpha_2 E^* I_2}{I_2^*} \left( \frac{E I_2^*}{E^* I_2} - 1 \right) + \frac{h_1 I_1^* I_2}{I_2^*} \left( \frac{I_1 I_2^*}{I_1^* I_3} - 1 \right), \\ \frac{dI_3}{dt} &= \frac{\alpha_3 E^* I_3}{I_3^*} \left( \frac{E I_3^*}{E^* I_3} - 1 \right) + \frac{h_2 I_1^* I_3}{I_3^*} \left( \frac{I_1 I_3^*}{I_1^* I_3} - 1 \right) + \frac{\lambda_1 I_2^* I_3}{I_3^*} \left( \frac{I_2 I_3^*}{I_2^* I_3} - 1 \right). \end{split}$$

Let us define the Lyapunov function as follows:

$$L = \left(S - S^* - S^* \ln \frac{S}{S^*}\right) + \left(E - E^* - E^* \ln \frac{E}{E^*}\right) + N_1 \left(I_1 - I_1^* - I_1^* \ln \frac{I_1}{I_1^*}\right)$$

$$+\,N_{2}\left(I_{2}-I_{2}^{*}-I_{2}^{*}\,ln\,\frac{I_{2}}{I_{2}^{*}}\right)+N_{3}\left(I_{3}-I_{3}^{*}-I_{3}^{*}\,ln\,\frac{I_{3}}{I_{3}^{*}}\right),$$

where

$$N_1 = \frac{\beta_1 S^* I_1^* + N_2 h_1 I_1^* + N_3 h_2 I_1^*}{\alpha_1 E^*}, \quad N_2 = \frac{\beta_2 S^* I_2^* + N_3 \lambda_1 I_2^*}{\alpha_2 E^* + h_1 I_1^*}, \quad N_3 = \frac{\beta_3 S^* I_3^*}{\alpha_3 E^* + h_2 I_1^* + \lambda_1 I_2^*}.$$

Next, the derivative of L with respect to time is calculated:

$$\begin{split} \frac{dL}{dt} &= \left(1 - \frac{S^*}{S}\right) \left[ S\left(\frac{\Lambda}{S^*} \left(\frac{S^*}{S} - 1\right) - \beta_1 I_1^* \left(\frac{I_1}{I_1^*} - 1\right) - \beta_2 I_2^* \left(\frac{I_2}{I_2^*} - 1\right) - \beta_3 I_3^* \left(\frac{I_3}{I_3^*} - 1\right) - \beta_4 E^* \left(\frac{E}{E^*} - 1\right) \right) \right] \\ &+ \left(1 - \frac{E^*}{E}\right) \left[ \frac{\beta_1 I_1^* S^* E}{E^*} \left(\frac{I_1 S E^*}{I_1^* S^* E} - 1\right) + \frac{\beta_2 I_2^* S^* E}{E^*} \left(\frac{I_2 S E^*}{I_2^* S^* E} - 1\right) \right] \\ &+ N_1 \left(1 - \frac{I_1^*}{I_1}\right) \left[ \frac{\alpha_1 E^* I_1}{I_1^*} \left(\frac{E I_1^*}{E^* I_1} - 1\right) \right] + N_2 \left(1 - \frac{I_2^*}{I_2}\right) \left[ \frac{\alpha_2 E^* I_2}{I_2^*} \left(\frac{E I_2^*}{E^* I_2} - 1\right) + \frac{h_1 I_1^* I_2}{I_2^*} \left(\frac{I_1 I_2^*}{I_1^* I_2} - 1\right) \right] \\ &+ N_3 \left(1 - \frac{I_3^*}{I_3}\right) \left[ \frac{\alpha_3 E^* I_3}{I_3^*} \left(\frac{E I_3^*}{E^* I_3} - 1\right) + \frac{h_2 I_1^* I_3}{I_3^*} \left(\frac{I_1 I_3^*}{I_1^* I_3} - 1\right) + \frac{\lambda_1 I_2^* I_3}{I_3^*} \left(\frac{I_2 I_3^*}{I_2^* I_3} - 1\right) \right], \\ &= \Lambda \left(2 - \frac{S}{S^*} - \frac{S}{S^*}\right) + \beta_1 S^* I_1^* \left(\frac{S}{S^*} - \frac{S I_1 E^*}{S^* I_1^* E}\right) + \beta_2 S^* I_2^* \left(\frac{S}{S^*} - \frac{S I_2 E^*}{S^* I_2^* E}\right) + \beta_3 S^* I_3^* \left(\frac{S}{S^*} - \frac{S I_3 E^*}{S^* I_3^* E}\right) \\ &+ N_1 \alpha_1 E^* \left(1 - \frac{E I_1^*}{E^* I_1}\right) + N_2 \alpha_2 E^* \left(1 - \frac{E I_2^*}{E^* I_2}\right) + N_2 h_1 I_1^* \left(1 - \frac{I_1 I_2^*}{I_1^* I_2}\right) + N_3 \alpha_3 E^* \left(1 - \frac{E I_3^*}{E^* I_3}\right) \\ &+ N_3 h_2 I_1^* \left(1 - \frac{I_1 I_3^*}{I_1^* I_3}\right) + N_3 \lambda_1 I_2^* \left(1 - \frac{I_1 I_3^*}{I_1^* I_3}\right) + N_3 \lambda_1 I_2^* \left(1 - \frac{I_2 I_3^*}{I_2^* I_3}\right). \end{split}$$

After substituting  $N_1$ ,  $N_2$ , and  $N_3$  into  $\frac{dL}{dt}$  and performing some algebraic manipulations, we obtain

$$\begin{split} \frac{\mathrm{dI}}{\mathrm{dt}} &= \Lambda \left(2 - \frac{S}{S^*} - \frac{S}{S^*}\right) + (\beta_1 S^* I_1 * + \beta_2 S^* I_2^*) \left(-2 + \frac{S^*}{S} + \frac{S}{S^*}\right) + \frac{\alpha_2 E^* \beta_2 S^* I_2^*}{\alpha_2 E^* + h_1 I_1^*} \left(3 - \frac{S^*}{S} - \frac{EI_2^*}{E^* I_2} - \frac{SI_2 E^*}{S^* I_2^* E}\right) \\ &+ \frac{h_1 I_1^* \beta_2 S^* I_2^*}{\alpha_2 E^* + h_1 I_1^*} \left(4 - \frac{S^*}{S} - \frac{EI_1^*}{E^* I_1} - \frac{I_1 I_2^*}{I_1^* I_2} - \frac{SI_2 E^*}{S^* I_3^* E}\right) + \frac{\beta_3 S^* I_3^* \alpha_3 E^*}{\alpha_3 E^* + h_2 I_1^* + \lambda_1 I_2^*} \left(3 - \frac{S^*}{S} - \frac{EI_3^*}{E^* I_3} - \frac{SI_2 E^*}{S^* I_3^* E}\right) \\ &+ \frac{\beta_3 S^* I_3^* (\alpha_3 E^* + h_2 I_1^*)}{\alpha_3 E^* + h_2 I_1^* + \lambda_1 I_2^*} \left(-2 + \frac{S^*}{S} + \frac{S}{S^*}\right) + \frac{\beta_3 S^* I_3^* h_2 I_1^*}{\alpha_3 E^* + h_2 I_1^* + \lambda_1 I_2^*} \left(4 - \frac{S^*}{S} - \frac{EI_3^*}{I_1^* I_3} - \frac{EI_1^*}{E^* I_1} - \frac{SI_2 E^*}{S^* I_3^* E}\right) \\ &+ \frac{\beta_3 S^* I_3^* h_2 I_1^*}{\alpha_3 E^* + h_2 I_1^* + \lambda_1 I_2^*} \left(-\frac{\lambda_1 I_2^*}{\alpha_2 E^* + h_1 I_1^*}\right) \left(-\frac{h_1 EI_1^{*2}}{E^* I_1} + \alpha_2 E^* - \frac{\alpha_2 EI_2^*}{I_2} + 2h_1 I_1^* - \frac{h_1 I_1 I_2^*}{I_2}\right) \\ &+ \lambda_1 I_2^* - \frac{\lambda_1 I_2 I_3^*}{I_3}\right) + \frac{\beta_3 SI_3^* \lambda_1 I_2^*}{\alpha_3 E^* + h_2 I_1^* + \lambda_1 I_2^*} - \frac{\beta_3 SI_3 E^* \lambda_1 I_2^*}{E(\alpha_3 E^* + h_2 I_1^* + \lambda_1 I_2^*)} \\ &\leq \Lambda \left(2 - \frac{S}{S^*} - \frac{S}{S^*}\right) + (\beta_1 S^* I_1 * + \beta_2 S^* I_2^* + \beta_3 S^* I_3^*) \left(-2 + \frac{S^*}{S} + \frac{S}{S^*}\right) \\ &+ \frac{\alpha_2 E^* \beta_2 S^* I_2^*}{\alpha_2 E^* + h_1 I_1^*} \left(3 - \frac{S^*}{S} - \frac{EI_2^*}{E^* I_2} - \frac{SI_2 E^*}{S^* I_2^* E}\right) + \frac{h_1 I_1^* \beta_2 S^* I_2^*}{\alpha_2 E^* + h_1 I_1^*} \left(4 - \frac{S^*}{S} - \frac{EI_1^*}{E^* I_1} - \frac{I_1 I_2^*}{I_1^* I_2} - \frac{SI_2 E^*}{S^* I_3^* E}\right) \\ &+ \frac{\beta_3 S^* I_3^* \alpha_3 E^*}{\alpha_3 E^* + h_2 I_1^* + \lambda_1 I_2^*} \left(3 - \frac{S^*}{S} - \frac{EI_3^*}{E^* I_3} - \frac{SI_3 E^*}{S^* I_3^*}\right) \\ &+ \frac{\beta_3 S^* I_3^* h_2 I_1^*}{\alpha_3 E^* + h_2 I_1^* + \lambda_1 I_2^*} \left(4 - \frac{S^*}{S} - \frac{EI_3^*}{E^* I_3} - \frac{SI_2 E^*}{S^* I_3^*}\right) \\ &+ \frac{\beta_3 S^* I_3^* h_2 I_1^*}{\alpha_3 E^* + h_2 I_1^* + \lambda_1 I_2^*} \left(4 - \frac{S^*}{S} - \frac{EI_3^*}{E^* I_3} - \frac{SI_2 E^*}{S^* I_3^*}\right) \\ &+ \frac{\beta_3 S^* I_3^* h_2 I_1^*}{\alpha_3 E^* + h_2 I_1^* + \lambda_1 I_2^*} \left(4 - \frac{S^*}{S} - \frac{EI_3^*}{E^* I_3} - \frac{EI_3^*}{E^* I_3}\right) \\ &+ \frac{\beta_3 S^* I_3^* h_2 I_1$$

From the equation (6.1), we can see that

$$\Lambda = \Big(\beta_1 I_1^* + \beta_2 I_2^* + \beta_3 I_3^* + \beta_4 E^*\Big) S^* + (\mu + \varphi_1) S^*.$$

Therefore, we obtain that

$$\begin{split} \frac{dL}{dt} &\leqslant \left( (\beta_4 \mathsf{E}^* + \mu + \varphi_1) \mathsf{S}^* \right) \left( 2 - \frac{S}{S^*} - \frac{S}{S^*} \right) + \frac{\alpha_2 \mathsf{E}^* \beta_2 \mathsf{S}^* \mathsf{I}_2^*}{\alpha_2 \mathsf{E}^* + h_1 \mathsf{I}_1^*} \left( 3 - \frac{S^*}{S} - \frac{\mathsf{E} \mathsf{I}_2^*}{\mathsf{E}^* \mathsf{I}_2} - \frac{\mathsf{S} \mathsf{I}_2 \mathsf{E}^*}{\mathsf{S}^* \mathsf{I}_2^* \mathsf{E}} \right) \\ &+ \frac{h_1 \mathsf{I}_1^* \beta_2 \mathsf{S}^* \mathsf{I}_2^*}{\alpha_2 \mathsf{E}^* + h_1 \mathsf{I}_1^*} \left( 4 - \frac{S^*}{S} - \frac{\mathsf{E} \mathsf{I}_1^*}{\mathsf{E}^* \mathsf{I}_1} - \frac{\mathsf{I}_1 \mathsf{I}_2^*}{\mathsf{I}_1^* \mathsf{I}_2} - \frac{\mathsf{S} \mathsf{I}_2 \mathsf{E}^*}{\mathsf{S}^* \mathsf{I}_3^* \mathsf{E}} \right) + \frac{\beta_3 \mathsf{S}^* \mathsf{I}_3^* \alpha_3 \mathsf{E}^*}{\alpha_3 \mathsf{E}^* + h_2 \mathsf{I}_1^* + \lambda_1 \mathsf{I}_2^*} \left( 3 - \frac{\mathsf{S}^*}{S} - \frac{\mathsf{E} \mathsf{I}_3^*}{\mathsf{E}^* \mathsf{I}_3} - \frac{\mathsf{S} \mathsf{I}_3 \mathsf{E}^*}{\mathsf{S}^* \mathsf{I}_3^* \mathsf{E}} \right) \\ &+ \frac{\beta_3 \mathsf{S}^* \mathsf{I}_3^* h_2 \mathsf{I}_1^*}{\alpha_3 \mathsf{E}^* + h_2 \mathsf{I}_1^* + \lambda_1 \mathsf{I}_2^*} \left( 4 - \frac{\mathsf{S}^*}{S} - \frac{\mathsf{I}_1 \mathsf{I}_3^*}{\mathsf{I}_1^* \mathsf{I}_3} - \frac{\mathsf{E} \mathsf{I}_1^*}{\mathsf{E}^* \mathsf{I}_1} - \frac{\mathsf{S} \mathsf{I}_3 \mathsf{E}^*}{\mathsf{S}^* \mathsf{I}_3^* \mathsf{E}} \right) \\ &+ \frac{\beta_3 \mathsf{S} \mathsf{I}_3^*}{\alpha_3 \mathsf{E}^* + h_2 \mathsf{I}_1^* + \lambda_1 \mathsf{I}_2^*} \left( \frac{\alpha_2 \mathsf{E}^* \lambda_1 \mathsf{I}_2^*}{\alpha_2 \mathsf{E}^* + h_1 \mathsf{I}_1^*} \left( 4 - \frac{\mathsf{E} \mathsf{I}_2^*}{\mathsf{E}^* \mathsf{I}_2} - \frac{\mathsf{I}_2 \mathsf{I}_3^*}{\mathsf{I}_2^* \mathsf{I}_3} - \frac{\mathsf{E}^*}{\mathsf{E}} - \frac{\mathsf{I}_3}{\mathsf{I}_3^*} \right) \right) \\ &+ \frac{h_1 \mathsf{I}_1^* \lambda_1 \mathsf{I}_2^*}{\alpha_2 \mathsf{E}^* + h_1 \mathsf{I}_1^*} \left( 5 - \frac{\mathsf{E} \mathsf{I}_1^*}{\mathsf{E}^* \mathsf{I}_1} - \frac{\mathsf{I}_1 \mathsf{I}_2^*}{\mathsf{I}_1^* \mathsf{I}_2} - \frac{\mathsf{I}_2 \mathsf{I}_3^*}{\mathsf{I}_2^* \mathsf{I}_3} - \frac{\mathsf{E}^*}{\mathsf{E}} - \frac{\mathsf{I}_3}{\mathsf{I}_3^*} \right) \right]. \end{split}$$

Thus, by applying the arithmetic-geometric mean inequality, we obtain  $\frac{dL}{dt} \leq 0$ . When  $R_0 > 1$ , we have  $\frac{dL}{dt} < 0$ . The equality  $\frac{dL}{dt} = 0$  holds if and only if  $S = S^*$ ,  $E = E^*$ ,  $I_1 = I_1^*$ ,  $I_2 = I_2^*$ ,  $I_3 = I_3^*$ ,  $I_4 = I_4^*$ , and  $R = R^*$ . According to LaSalle's invariance principle [19], the endemic equilibrium  $\varepsilon^*$  is globally asymptotically stable when  $R_0 > 1$ .

# 7. Optimal control study

Our initial model has already integrated the initial measures implemented by the Thailand Public Health Administration, which we have analyzed using available data. Conducting an optimal control study is valuable for exploring intervention policies aimed at achieving specific objectives, whether it be minimizing or maximizing the problem of interest. This approach serves as a useful tool for future reference, particularly in the event of similar historic occurrences. However, in our initial model, the parameters for intervention measures are estimated as constants, remaining unchanged over time. This lack of temporal variation could potentially lead to an overemphasis on certain aspects in real-world scenarios. In this section, our focus centers on determining the optimal implementation of control strategies encompassing the vaccination rate of susceptible individuals  $(u_1(t))$ , control measures such as wearing masks, home isolation, social distancing, and providing healthcare for exposed and infectious individuals  $(u_2(t))$ , treatment rates for infected individuals in field hospitals (u<sub>3</sub>(t)), treatment rates for infected individuals in ICU without oxygen tubes  $(u_4(t))$ , and treatment rates for infected individuals in ICU with oxygen tubes  $(u_5(t))$ . These strategies aim to minimize the total number of infectious individuals while simultaneously minimizing associated control costs. We adjust model (2.1)-(2.7) by integrating time-dependent control variables  $\phi_i = u_i(t)$ , where i ranges from 1 to 5. Thus, the COVID-19 model (2.1)-(2.7) with time-dependent controls (measured in days) is expressed as follows:

$$\frac{dS}{dt} = \Lambda - (\beta_1 I_1 + \beta_2 I_2 + \beta_3 I_3 + \beta_4 E) S - (\mu + u_1(t)) S, \tag{7.1}$$

$$\frac{dE}{dt} = \left(\beta_{1}I_{1} + \beta_{2}I_{2} + \beta_{3}I_{3} + \beta_{4}E\right)S - (\alpha_{1} + \alpha_{2} + \alpha_{3} + \alpha_{4} + \mu + \gamma_{5} + u_{2}(t))E, \tag{7.2}$$

$$\frac{dI_1}{dt} = \alpha_1 E - (\mu + d_1 + \gamma_1 + h_1 + h_2 + h_3 + u_3(t))I_1, \tag{7.3}$$

$$\frac{dI_2}{dt} = \alpha_2 E + h_1 I_1 - (\mu + d_2 + \gamma_2 + \lambda_1 + \lambda_2 + u_4(t)) I_2, \tag{7.4}$$

$$\frac{dI_3}{dt} = \alpha_3 E + h_2 I_1 + \lambda_1 I_2 - (\mu + d_3 + \gamma_3 + \varepsilon + u_5(t)) I_3, \tag{7.5}$$

$$\frac{dI_4}{dt} = \alpha_4 E + h_3 I_1 + \lambda_2 I_2 + \varepsilon I_3 - (\mu + d_4 + \gamma_4) I_4, \tag{7.6}$$

$$\frac{dR}{dt} = u_1(t)S + (\gamma_1 + u_3(t))I_1 + (\gamma_2 + u_4(t))I_2 + (\gamma_3 + u_5(t))I_3 + \gamma_4 I_4 + (\gamma_5 + u_2(t))E - \mu R.$$
 (7.7)

We consider the system over a time interval [0,T]. The functions  $u_1(t)$ ,  $u_2(t)$ ,  $u_3(t)$ ,  $u_4(t)$ , and  $u_5(t)$  are assumed to be at least Lebesgue measurable on [0,T]. We now introduce the following objective functional:

$$\begin{split} J(u_1^*,u_2^*,u_3^*,u_4^*,u_5^*) &= min \int_0^T [E+I_1+I_2+I_3+I_4+c_1u_1(t)S+c_2u_2(t)E+c_3u_3(t)I_1 \\ &+ c_4u_4(t)I_2+c_5u_5(t)I_3 + \frac{1}{2} \left(c_6u_1^2(t)+c_7u_2^2(t)+c_8u_3^2(t)+c_9u_4^2(t)+c_{10}u_5^2(t)\right) ] \; dt, \end{split}$$

where,  $c_i$  (where i=1,2,3,4,5) represents the respective positive balancing constants, while the terms  $c_6u_1^2(t)$ ,  $c_7u_2^2(t)$ ,  $c_8u_3^2(t)$ ,  $c_9u_4^2(t)$ , and  $c_{10}u_5^2(t)$  denote the costs associated with vaccination control, treatment of infected people in field hospitals, treatment of infected people in ICU without an oxygen tube, and treatment of infected people in ICU with an oxygen tube, respectively. This objective function aims to minimize the total number of exposed, infectious, and other infected individuals while keeping the intervention costs as low as possible. The Hamiltonian (H) for the objective functional J is derived by applying Pontryagin's Minimum Principle, as described in [35]. It is given by

$$\begin{split} \mathsf{H} &= \mathsf{E} + \mathsf{I}_1 + \mathsf{I}_2 + \mathsf{I}_3 + \mathsf{I}_4 + c_1 u_1(t) \mathsf{S} + c_2 u_2(t) \mathsf{E} + c_3 u_3(t) \mathsf{I}_1 + c_4 u_4(t) \mathsf{I}_2 \\ &+ c_5 u_5(t) \mathsf{I}_3 + \frac{1}{2} \left( c_6 u_1^2(t) + c_7 u_2^2(t) + c_8 u_3^2(t) + c_9 u_4^2(t) + c_{10} u_5^2(t) \right) \right) \\ &+ \lambda_S \left[ \Lambda - \left( \beta_1 \mathsf{I}_1 + \beta_2 \mathsf{I}_2 + \beta_3 \mathsf{I}_3 + \beta_4 \mathsf{E} \right) \mathsf{S} - (\mu + u_1(t)) \mathsf{S} \right] \\ &+ \lambda_E \left[ \left( \beta_1 \mathsf{I}_1 + \beta_2 \mathsf{I}_2 + \beta_3 \mathsf{I}_3 + \beta_4 \mathsf{E} \right) \mathsf{S} - (\alpha_1 + \alpha_2 + \alpha_3 + \alpha_4 + \mu + \gamma_5 + u_2(t)) \mathsf{E} \right] \\ &+ \lambda_{\mathsf{I}_1} \left[ \alpha_1 \mathsf{E} - (\mu + d_1 + \gamma_1 + h_1 + h_2 + h_3 + u_3(t)) \mathsf{I}_1 \right] \\ &+ \lambda_{\mathsf{I}_2} \left[ \alpha_2 \mathsf{E} + h_1 \mathsf{I}_1 - (\mu + d_2 + \gamma_2 + \lambda_1 + \lambda_2 + u_4(t)) \mathsf{I}_2 \right] \\ &+ \lambda_{\mathsf{I}_3} \left[ \alpha_3 \mathsf{E} + h_2 \mathsf{I}_1 + \lambda_1 \mathsf{I}_2 - (\mu + d_3 + \gamma_3 + \varepsilon + u_5(t)) \mathsf{I}_3 \right] \\ &+ \lambda_{\mathsf{I}_4} \left[ \alpha_4 \mathsf{E} + h_3 \mathsf{I}_1 + \lambda_2 \mathsf{I}_2 + \varepsilon \mathsf{I}_3 - (\mu + d_4 + \gamma_4) \mathsf{I}_4 \right] \\ &+ \lambda_{\mathsf{R}} \left[ u_1(t) \mathsf{S} + (\gamma_1 + u_3(t)) \mathsf{I}_1 + (\gamma_2 + u_4(t)) \mathsf{I}_2 + (\gamma_3 + u_5(t)) \mathsf{I}_3 + \gamma_4 \mathsf{I}_4 + (\gamma_5 + u_2(t)) \mathsf{E} - \mu \mathsf{R} \right]. \end{split}$$

Given an optimal control  $u_1^*(t)$ ,  $u_2^*(t)$ ,  $u_3^*(t)$ ,  $u_4^*(t)$ , and  $u_5^*(t)$ , there exist adjoint functions,  $\lambda_S$ ,  $\lambda_E$ ,  $\lambda_{I_1}$ ,  $\lambda_{I_2}$ ,  $\lambda_{I_3}$ ,  $\lambda_{I_4}$ , and  $\lambda_R$ , corresponding to the states S, E,  $I_1$ ,  $I_2$ ,  $I_3$ ,  $I_4$ , and R, respectively, that satisfy:

$$\begin{split} \frac{d\lambda_S}{dt} &= -\frac{\partial H}{\partial S} = -\left[c_1u_1(t) + \lambda_S(-(\beta_1I_1 + \beta_2I_2 + \beta_3I_3 + \beta_4E) - \mu - u_1(t)) \right. \\ &\quad + \lambda_E(\beta_1I_1 + \beta_2I_2 + \beta_3I_3 + \beta_4E) + \lambda_Ru_1(t) \bigg], \\ \frac{d\lambda_E}{dt} &= -\frac{\partial H}{\partial E} = -\left[1 + c_2u_2(t) + \lambda_S(-\beta_4S) + \lambda_E(\beta_4S - (\alpha_1 + \alpha_2 + \alpha_3 + \alpha_4 + \mu + \gamma_5) \right. \\ &\quad - u_2(t)) + \lambda_{I_1}\alpha_1 + \lambda_{I_2}\alpha_2 + \lambda_{I_3}\alpha_3 + \lambda_{I_4}\alpha_4 + \lambda_R(\gamma_5 + u_2(t)) \bigg], \\ \frac{d\lambda_{I_1}}{dt} &= -\frac{\partial H}{\partial I_1} = -\left[1 + c_3u_3(t) + \lambda_E\beta_1S + \lambda_{I_1}(-(\mu + d_1 + \gamma_1 + h_1 + h_2 + h_3) - u_3(t)) \right. \\ &\quad + \lambda_{I_2}h_1 + \lambda_{I_3}h_2 + \lambda_{I_4}h_3 + \lambda_R(\gamma_1 + u_3(t)) \bigg], \end{split}$$

$$\begin{split} \frac{d\lambda_{I_2}}{dt} &= -\frac{\partial H}{\partial I_2} = -\left[1 + c_4 u_4(t) + \lambda_{I_2}(-(\mu + d_2 + \gamma_2 + \lambda_1 + \lambda_2) - u_4(t)) + \lambda_{I_3} \lambda_1 + \lambda_{I_4} \lambda_2 + \lambda_R(\gamma_2 + u_4(t))\right], \\ \frac{d\lambda_{I_3}}{dt} &= -\frac{\partial H}{\partial I_3} = \left[1 + c_5 u_5(t) + \lambda_{I_3}(-(\mu + d_3 + \gamma_3 + \varepsilon) - u_5(t)) + \lambda_{I_4} \varepsilon + \lambda_R(\gamma_3 + u_5(t))\right], \\ \frac{d\lambda_{I_4}}{dt} &= -\frac{\partial H}{\partial I_4} = -\left[1 + \lambda_{I_4}(-(\mu + d_4 + \gamma_4)) + \lambda_R \gamma_4\right], \\ \frac{d\lambda_R}{dt} &= -\frac{\partial H}{\partial R} = -\left[\lambda_R(-\mu)\right]. \end{split}$$

With the transversality conditions,  $\lambda_S(T)=0$ ,  $\lambda_E(T)=0$ ,  $\lambda_{I_1}(T)=0$ ,  $\lambda_{I_2}(T)=0$ ,  $\lambda_{I_3}(T)=0$ ,  $\lambda_{I_4}(T)=0$ , and  $\lambda_R(T)=0$ . The characterizations of the optimal controls  $u_i(t)$  for i=1,2,3,4,5 are then based on the conditions:

$$\frac{\partial H}{\partial u_{i}} = 0$$
, where  $i = 1, 2, 3, 4, 5$ ,

subject to the constraints  $0 \leqslant u_i(t) \leqslant u_{i\,max}$ , for i=1,2,3,4,5. Moreover, the optimal controls are characterized by the following optimality conditions:

$$u_i^*(t) = \text{max}\{0, \text{min}\{u_i(t), u_{i\,\text{max}}\}\},$$

where

$$\begin{split} u_1(t) &= \frac{\lambda_S S - \lambda_R S - c_1 S}{c_6}, \qquad \quad u_2(t) = \frac{\lambda_E E - \lambda_R E - c_2 E}{c_7}, \qquad \quad u_3(t) = \frac{\lambda_{I_1} I_1 - \lambda_R I_1 - c_3 I_1}{c_8}, \\ u_4(t) &= \frac{\lambda_{I_2} I_2 - \lambda_R I_2 - c_4 I_2}{c_9}, \qquad \quad u_5(t) = \frac{\lambda_{I_3} I_3 - \lambda_R I_3 - c_5 I_3}{c_{10}}. \end{split}$$

#### 8. Numerical results

In late 2020, Thailand began its vaccine distribution policy, initially focusing on a limited segment of the population. By around October 2021, the country expanded its vaccination efforts to encompass broader segments of society, alongside implementing additional strategies such as home isolation, social distancing, and mask-wearing. During the fourth wave of infections, nearly half of the population received their first vaccine dose [10]. However, the successful control of the disease in Thailand may have been attributed to a combination of various strategies. In this simulation, we aim to investigate these strategies by considering the initial intervention policies implemented by Thailand.

Initially, during the second and third waves of infections (February 2021-July 2021), Thailand vaccinated only about 2-5 percent of the population, with no vaccines available during the first wave. By the third wave, the vaccination rate increased to approximately 30 percent of the population, albeit progressing slowly due to limited vaccine availability. During the fourth wave, Thailand ramped up its vaccination efforts, vaccinating around 15 percent of the population by mid-July and reaching approximately 70 percent by the end of December 2021. On average, Thailand administered vaccines at a rate of 0.4 percent of the population daily during this period. However, for the entire duration of the fourth wave, the average daily vaccination rate should ideally range between 0.05 to 0.4 percent of the population. Therefore, the initial vaccination rate ( $\phi_1$ ) for Thailand during this period is estimated to be approximately 0.05 to 0.4 percent daily [8].

During the fourth wave, individuals who were exposed or infectious were required to self-isolate. Thailand also faced shortages of essential medical supplies, masks, and basic healthcare for COVID-19 patients. Consequently, the estimation of the availability of these measures ( $\phi_2$ ) ranged between 10 to 20 percent. Thailand established "field hospitals" to offer temporary care for infectious individuals with mild to moderate symptoms, overseen by regular hospitals. The control measures for this group were estimated to range between 40 to 60 percent, considering the surveillance and treatment provided. As the

number of individuals in intensive care units (ICUs) was relatively small and had minimal impact on the reproduction number, the control rates for this aspect were relatively low. The values of other parameters are listed in Table 2.

Table 2: Parameter values.							
Symbol	Value	Reference	Symbol	Value	Reference		
N	71800000	[10]	$I_0$	26	[9]		
$h_1$	0.000168	[14]	$d_1$	$3.765 \times 10^{-5}$	Estimated		
$h_2$	0.00001	Assumed	$d_2$	0.0014286	Assumed		
$h_3$	0.0000001	Assumed	$d_3$	0.0010143	[39]		
$\lambda_1$	0.001	Assumed	$\mathrm{d}_4$	0.0001143	Assumed		
$\lambda_2$	0.0001	Assumed	$\gamma_1$	[0.00284 - 0.2]	[14]		
$\epsilon$	0.00001	Assumed	$\gamma_2$	[0.0075 - 0.2]	Estimated		
$\alpha_1$	0.01267	<b>Estimated</b>	γ3	[0.0026 - 0.0833]	<b>Estimated</b>		
$\alpha_2$	0.0012 - 0.1	Estimated	$\gamma_4$	0.001	Estimated		
$\alpha_3$	0.0120 - 0.1	Assumed	$\gamma_5$	0.01819	[14]		
$lpha_4$	0.0120	Assumed	$\phi_1$	[0.0005 - 0.004]	Estimated		
$\beta_1$	$5.571 \times 10^{-12}$	Estimated	$\phi_2$	0.125	Estimated		
$\beta_2$	$1.3928 \times 10^{-13}$	Estimated	$\phi_3$	0.4	Estimated		
$\beta_3$	$1.3928 \times 10^{-15}$	Assumed	$\phi_4$	0.00001	Assumed		
$eta_4$	$4.1783 \times 10^{-9}$	Estimated	Ф5	0.00001	Assumed		
Λ	$\frac{273523621}{65 \times 365}$	[43]	μ	$\frac{1}{65\times365}$	[43]		

Please note that the infection rates listed in Table 2 are estimated based on the curve fitting technique using data from Thailand. To estimate  $\beta_1$ ,  $\beta_2$ ,  $\beta_3$ ,  $\beta_4$ ,  $\gamma_1$ ,  $\gamma_2$ ,  $\gamma_3$ ,  $\gamma_4$ , and  $\gamma_5$ , we used the curve fitting technique by using the Trust Region Reflective (TRF) method for the bound parameters. The calculation yielded an RMSE of 2,487.1732 cases between the real data and the model. The model produced a root mean square error (RMSE) of 2,487.1732 cases when compared with the observed data. Given a total susceptible population of 71,800,000 individuals, this corresponds to a relative error of approximately 0.0035%. Although the absolute error appears large, it is negligible when expressed as a proportion of the population, indicating that the model provides a strong fit to the observed data at the population scale. Figure 4 shows the real data and the fitted curve of our model. This fit gives the parameters listed in Table 2. Additionally, we have compared these values with those from other research papers, finding that they are calculated similarly and yield comparable results. For example, while the average recovery time for infected individuals is typically 4 days, during this wave of the outbreak in Thailand, it has increased to an average of 6 days. Therefore, the recovery rate may show slight variations. Some parameters are assumed due to the unavailability of data; however, these assumptions are based on epidemiological reasoning.

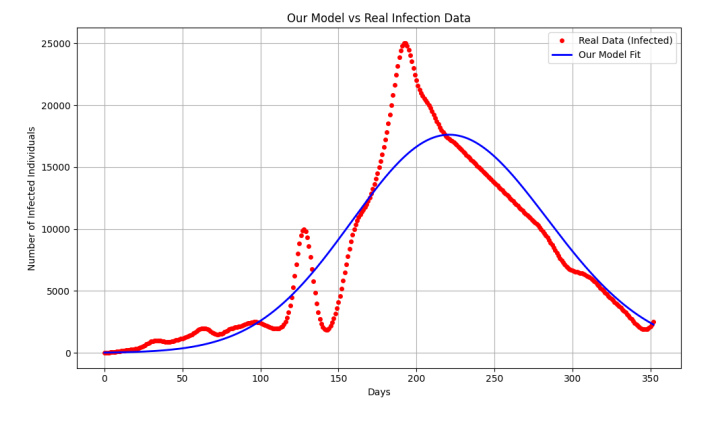


Figure 4: Parameter estimation using real data and the fitted model.

In this section, we employ the forward-backward sweep method to numerically solve the optimality of the system. In MATLAB code, the state variables are represented by x(t), the adjoint functions by  $\lambda(t)$ , and the control variables by u(t). For the forward-backward method, we follow these steps. For  $0 \le t \le t_1$ ,

- Step 1. Make an initial guess for u(t) over the given interval and store it as u(t).
- Step 2. Using the initial condition x(t) and the stored values for u, solve x(t) forward in time according to its differential equation in the optimality system.
- Step 3. Using the transversality condition  $\lambda(t_1)=0$  and the stored values for u(t) and x(t), solve  $\lambda(t)$  backward in time according to its differential equation in the optimality system.
- Step 4. Update the control by substituting the new x(t) and  $\lambda$  values into the characterization of u.
- Step 5. Check convergence. If the difference between the variable values in the current and previous iterations is negligibly small, output the current values as the solution. If not, return to Step 2 and repeat the process.

For Steps 2 and 3, any ODE solver can be used. In our case, we chose Euler's method since the system is not overly complex. For our computational work, we used MATLAB version R2024b.

Initially, we adjust the parameter values to align with the data provided in Table 2. To investigate the intervention policies distributed by the Thailand Public Health Administration and compare with our scenarios, we show each case study as follows.

# 8.1. Case study 1: actual public health interventions and model fitting for optimal control model

On average, we estimated that Thailand vaccinated susceptible individuals at a rate of 0.001 per day (equivalent to 0.1 percent of the susceptible population per day). Therefore, for the initial model with constant vaccination measures ( $\phi_1$ ), we set  $\phi_1 = 0.001$ . As shown in Table 2, we estimated other measure values. At the time of detecting COVID-19, Thailand had a total population of approximately 71,800,000 people, with authorities confirming 26 infectious cases. Hence, we set the initial conditions as follows:  $(S(0), E(0), I_1(0), I_2(0), I_3(0), R(0))$  as (71800000, 26, 0, 0, 0, 0, 0).

To compare with a constant intervention strategy, we investigate an optimal control problem where the maximum vaccine effort  $(u_{1_{max}})$  that can be deployed is set at a rate of 0.001 per day, matching the actual average distributed by the Thai Public Health Administration. The government prioritizes preventing and reducing the number of infections as the first priority, followed by considering the cost of vaccination. Distributing other measures is deemed equally important to maintaining the number of each state low. Therefore, we assign weighting constants  $c_1 = 0.0001$ ,  $c_2 = 1$ ,  $c_3 = 1$ ,  $c_4 = 1$ ,  $c_5 = 1$ ,  $c_6 = 2$ ,  $c_7 = 2$ ,  $c_8 = 2$ ,  $c_9 = 2$ , and  $c_{10} = 2$ . Additionally, the corresponding basic reproduction number is approximately 3.03.

Figure 6 (a) illustrates the trajectory of exposed and infectious individuals under constant measures (with a vaccination rate of 0.1 percent of susceptible per day). However, the current control measures in place are inadequate to curb the COVID-19 outbreak, leading to a significant number of infections (peaking at approximately 25,000 new infections). Indeed, the infection trend depicted here closely resembles the real data from the Thai Public Health Administration, as shown in Figure 5. Additionally, other categories of individuals have been plotted for further investigation, as depicted in Figure 6.

Figure 7 illustrates the optimal control measure model, where (a) showcases the trajectory of the number of exposed and infectious individuals (E), reaching a peak of approximately 25,000 cases around day 210 before gradually declining to zero by the year's end. Additionally, Figure 7 (b) demonstrates that, with the implementation of controls, the number of infectious individuals treated in field hospitals peaks at around 160. Similarly, Figures 7 (c) and 7 (d) indicate that the numbers of infectious individuals receiving treatment in the ICU without oxygen tubes and with oxygen tubes remain very small. Consequently, in this scenario, if all controls are enacted as depicted in Figure 8, the numbers of individuals in the ICU and critical condition remain low.

The optimal control profiles suggest that to achieve the same goal (number of new infections) as the actual control measures implemented, as shown in Figure 9, vaccination should be administered at a rate of 0.001 (or 0.1 percent) of the susceptible population per day for the entire year, resulting in approximately 36.5 percent of the population being vaccinated by the year's end. Additionally, other measures should follow suit, as depicted in Figure 8.

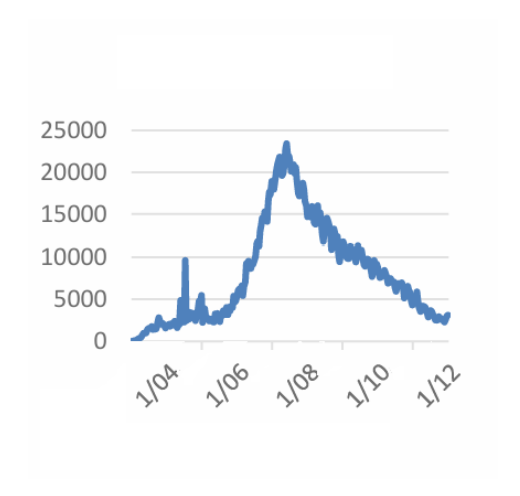


Figure 5: Thailand's infection report during the fourth wave [10].

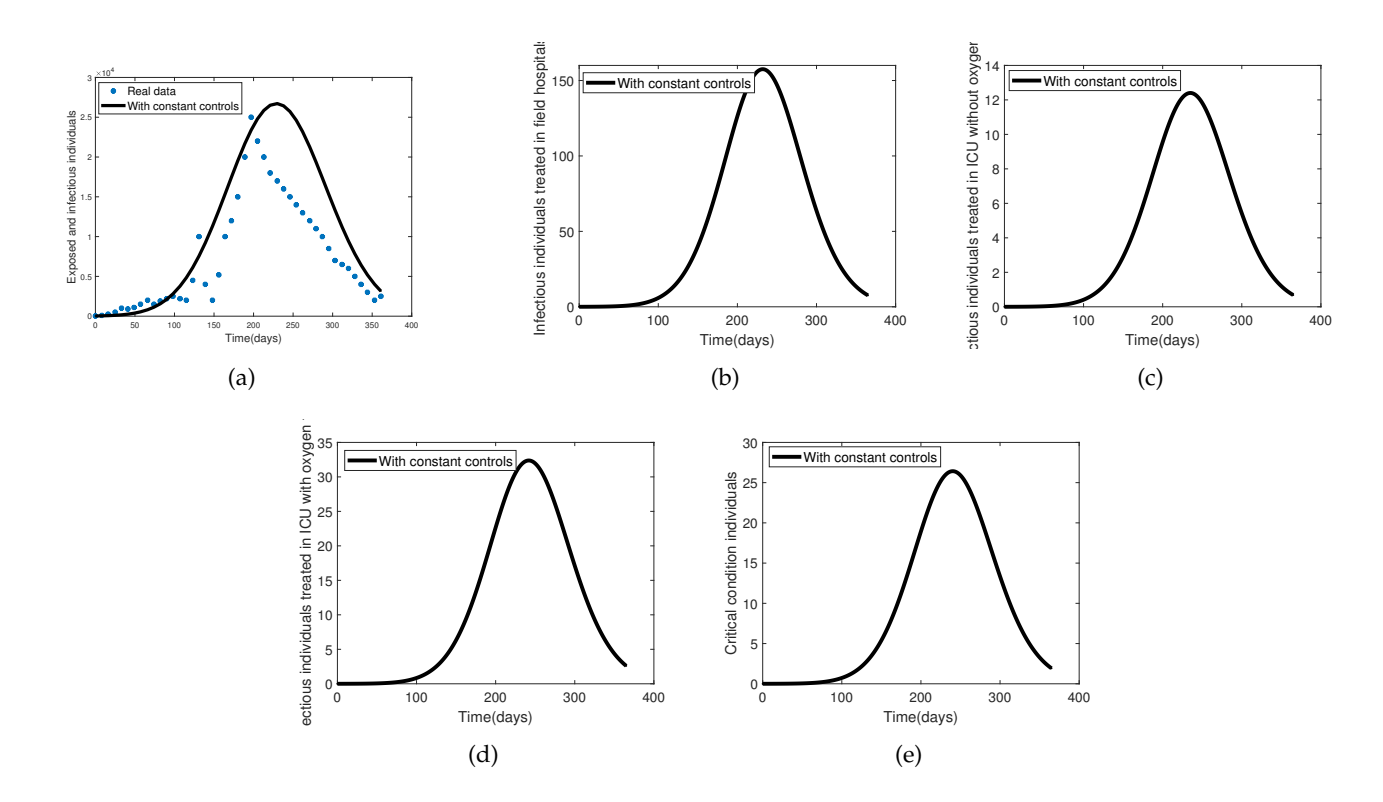


Figure 6: The simulation results of the model cover scenarios with constant controls for: (a) exposed and infectious individuals; (b) infectious individuals treated in field hospitals; (c) infectious individuals treated in the ICU without oxygen tubes; (d) infectious individuals treated in the ICU with oxygen tubes; and (e) individuals in critical condition.

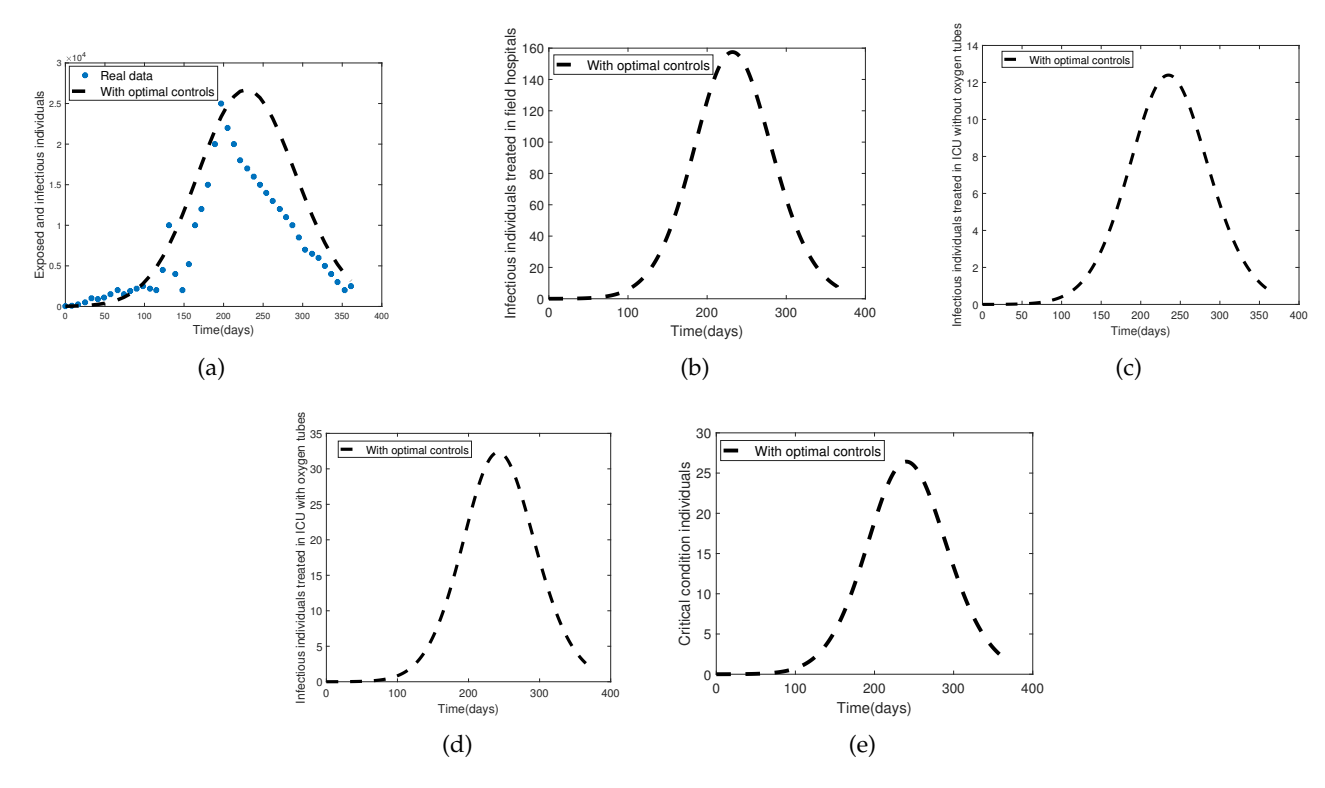


Figure 7: The simulation results of the model cover scenarios with optimal controls for: (a) exposed and infectious individuals; (b) infectious individuals treated in field hospitals; (c) infectious individuals treated in the ICU without oxygen tubes; (d) infectious individuals treated in the ICU with oxygen tubes; and (e) individuals in critical condition.

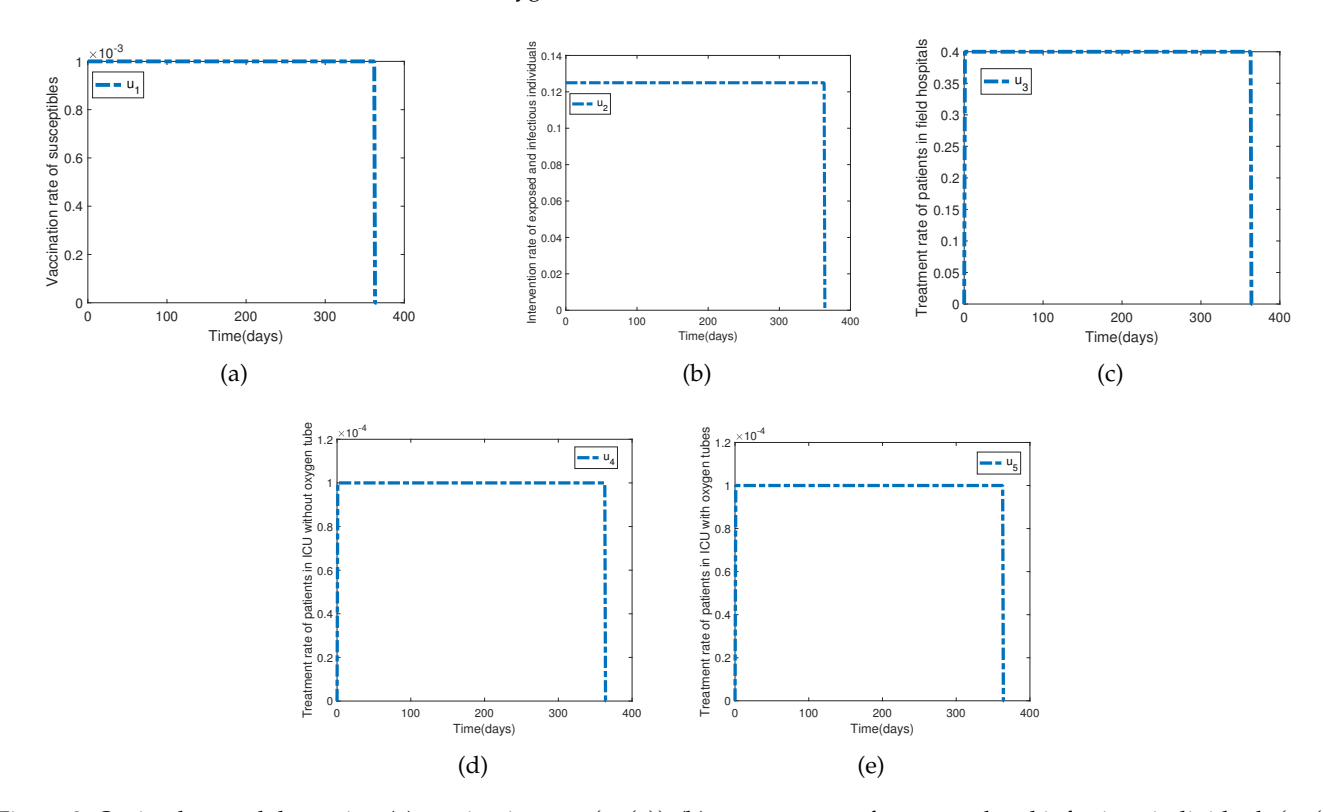


Figure 8: Optimal control dynamics: (a) vaccination rate  $(u_1(t))$ ; (b) treatment rate for exposed and infectious individuals  $(u_2(t))$ ; (c) treatment rate for infected individuals in field hospitals  $(u_3(t))$ ; (d) treatment rate for infected individuals in the ICU without oxygen tubes  $(u_4(t))$ ; and (e) treatment rate for infected individuals in the ICU with oxygen tubes  $(u_5(t))$ .

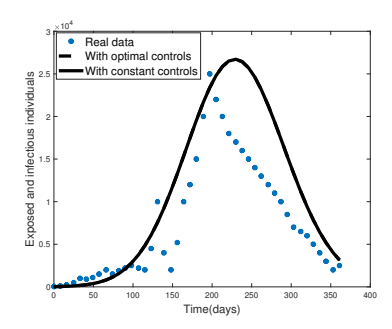


Figure 9: When comparing the constant measures implemented by the Thailand Public Health Administration with the optimal control model, we find that the number of new infections in both models is quite similar. Their curves overlap, effectively representing the trends in the number of exposed and infectious individuals.

# 8.2. Case study 2: achieving 70 percent vaccination of the susceptible population in one year with constant measure costs

In this simulation, we assume that Thailand achieves its goal of vaccinating about 73 percent (0.2 percent per day) of the susceptible population at the end of the year, disregarding the cost of vaccination, while maintaining other measures. As shown in Figure 10, without optimal controls (with control measures remaining constant each day), the number of new infections (exposed and infectious) decreases dramatically, peaking at 110 days with only 800 infected individuals, as illustrated in Figure 10(a). This result is comparable to the optimal control model (not shown here), with the number of new infections for both models (constant controls and optimal controls) being relatively the same, as shown in Figure 11. We will not show the real data for this case due to the significant difference between the numbers of real data and simulated results.

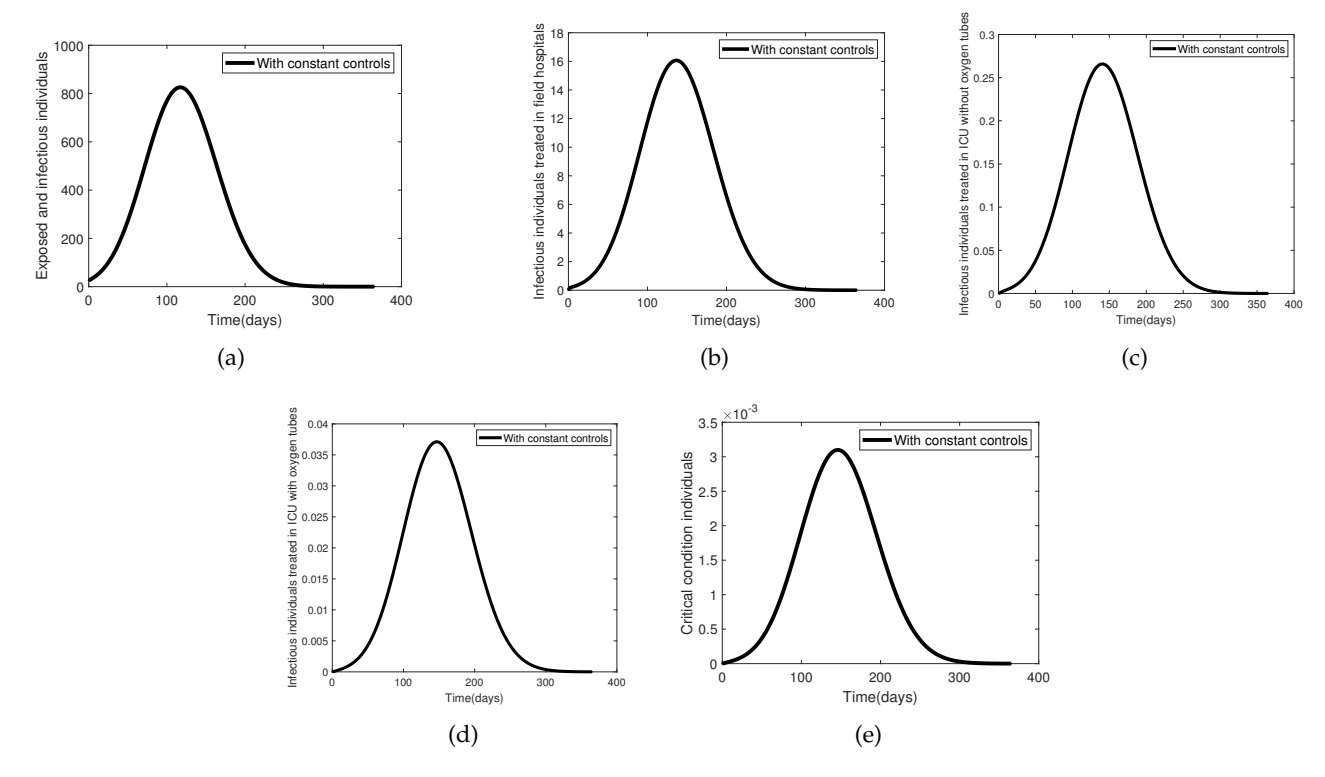


Figure 10: The simulation results of the model cover scenarios with constant controls for (a) exposed and infectious individuals; (b) infectious individuals treated in ICUs without oxygen tubes; (d) infectious individuals treated in ICUs with oxygen tubes; and (e) individuals in critical condition.

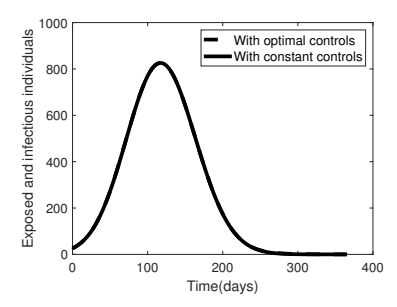


Figure 11: With the assumed constant measures implemented by the Thailand Public Health Administration (vaccinating 73 percent of susceptible individuals per year) compared to optimal control strategies, we observe that the number of new infections in both models is relatively similar, with their curves overlapping.

The optimal control profiles for this case study are presented in Figure 12. Figure 12(a) indicates that about 0.2 percent of the susceptible population should be vaccinated each day, allowing the vaccination program to conclude around day 230 after the first day of vaccination (46 percent in total), rather than continuing at the same rate throughout the entire year as in the constant control model.

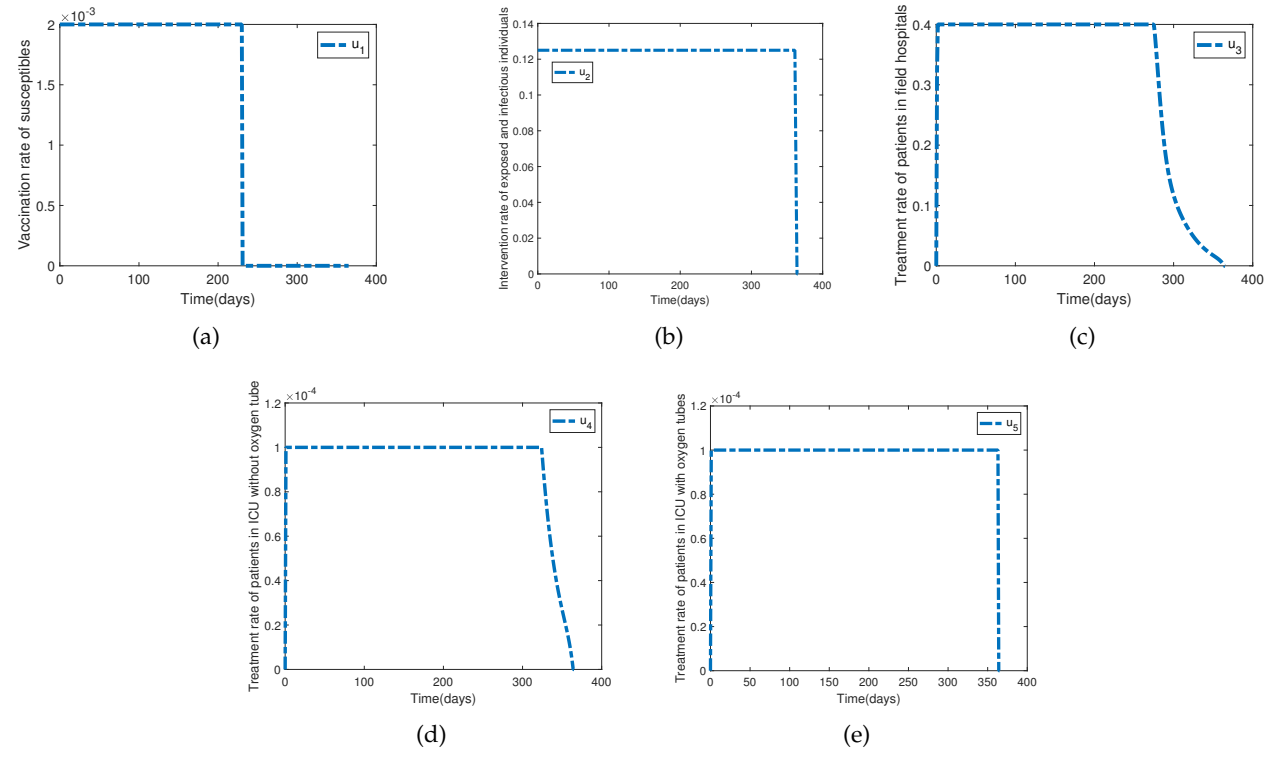
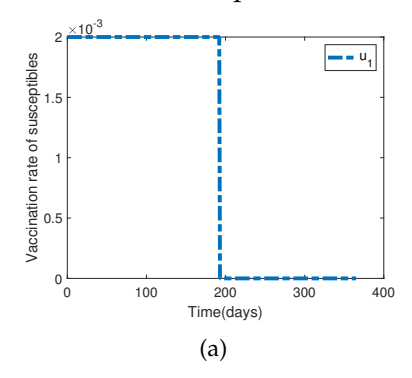


Figure 12: Optimal control dynamics for the case study: (a) vaccination rate  $(u_1(t))$ ; (b) treatment rate for exposed and infectious individuals  $(u_2(t))$ ; (c) treatment rate for infected individuals in field hospitals  $(u_3(t))$ ; (d) treatment rate for infected individuals in the ICU without oxygen tubes  $(u_4(t))$ ; and (e) treatment rate for infected individuals in the ICU with oxygen tubes  $(u_5(t))$ .

Next, we consider increasing the vaccination cost slightly by adjusting the weight parameter  $c_1$  from 0.0001 to 0.001. According to our simulations, this adjustment results in a shorter distribution period for the optimal vaccination control measure, reducing it from 230 to 180 days, as depicted in Figure 13(a). Additionally, we observe that the number of new infections for the optimal control problem is slightly higher than that of the constant control model. This discrepancy arises because there are no further vaccinations administered after the 180th day, as illustrated in Figure 13(b).

This strategy indicates that rather than vaccinating the susceptible population for the entire year, a duration of approximately 180 days may suffice, offering potential cost savings. However, this simulated results are based on the assumption that vaccination must be deployed at 0.2 percent of the susceptible population per day. Although the simulated results suggest that 230 days should be sufficient for vac-

cination, in reality, the program should continue until at least 70% of the population is covered, as the simulations are based on assumed parameters.



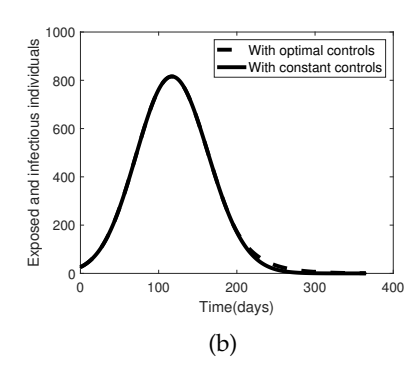


Figure 13: The simulation reveals (a) the vaccination rate for the optimal control problem; (b) when comparing the constant measures implemented by the Thailand Public Health Administration to optimal control strategies, we observe that the number of new infections for both models is relatively consistent, with their curves overlapping.

# 8.3. Case study 3: contrasting real constant control measures plus assumed additional measures with optimal control strategies

In this section, our focus is on exploring how Thailand could enhance its disease control efforts by incorporating additional measures alongside a vaccination plan targeting only 0.1 percent of the susceptible population per day. The simulations are based on observed circumstances from Thailand's Public Health Intervention program and the number of infected cases during the outbreak period. Once again, we will not present the real data for this case due to the substantial discrepancy between the actual figures and the simulated results.

We hypothesize that implementing successful policies to prevent exposed individuals from spreading the disease to susceptible populations, such as reducing parameter  $\beta_4$  from 0.3 divided by the total population to 0.25 divided by the total population, coupled with measures like wearing masks, social distancing, and encouraging infected individuals to stay home, could lead to significant outcomes. Figure 14 (a) illustrates a significant reduction in the number of exposed individuals, with a peak of only about 35 individuals on day 50 after the onset of the outbreak. Similarly, Figure 14 (b) shows a decrease in the number of infected individuals treated in field hospitals.

To achieve these outcomes, authorities should implement control measures to support exposed individuals in staying indoors, provide medical assistance for those with mild symptoms, and promote mask-wearing and social distancing. Figures 14 (c), (d), and (e) demonstrate similar trends for other states regarding exposed and infectious individuals treated in field hospitals, indicating a reduction in numbers as well.

The optimal control measures for this simulation are outlined in Figure 15. In Figure 15 (a), the vaccination policy for susceptible populations is deployed over approximately 150 days instead of the entire year. Other controls are depicted in Figures 15 (b), (c), (d), and (e). The optimal control guideline emphasizes the importance of vaccination policies for the initial 150 days, during which other measures can be minimal to prevent the escalation of infections.

The simulation results of constant controls are shown in Figure 16, and the comparison between the constant control model and the optimal control model is represented in Figure 17. The tail of the optimal control model is slightly higher than that of the constant control model, primarily because the vaccination policy in the optimal control model ceases around day 150.

It's important to note that while the data collected during the COVID-19 outbreak in 2021-2022 categorized infected individuals, which we used to formulate equations capturing the dynamic behaviors of the disease and the population, our simulations may slightly deviate from the actual data in terms of total individuals in each state. Nonetheless, these simulations offer valuable insights, demonstrating how strategic deployment of intervention programs can help in reducing and controlling the spread of COVID-19.

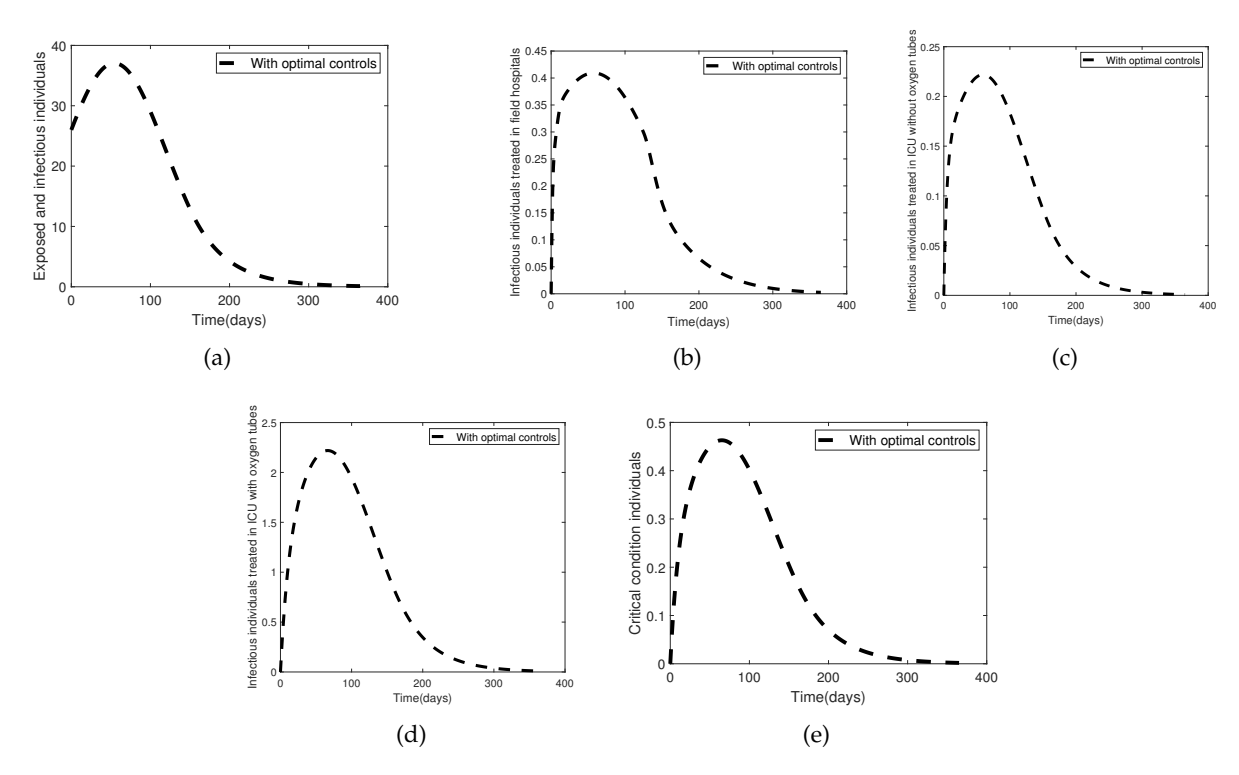


Figure 14: The simulation results of the model encompass scenarios with optimal controls aimed at reducing the transmission rate from exposed infectious individuals to susceptible population for (a) exposed and infectious individuals; (b) infectious individuals treated in ICU without oxygen tube; (d) infectious individuals treated in ICU with oxygen tubes; and (e) individuals in critical condition.

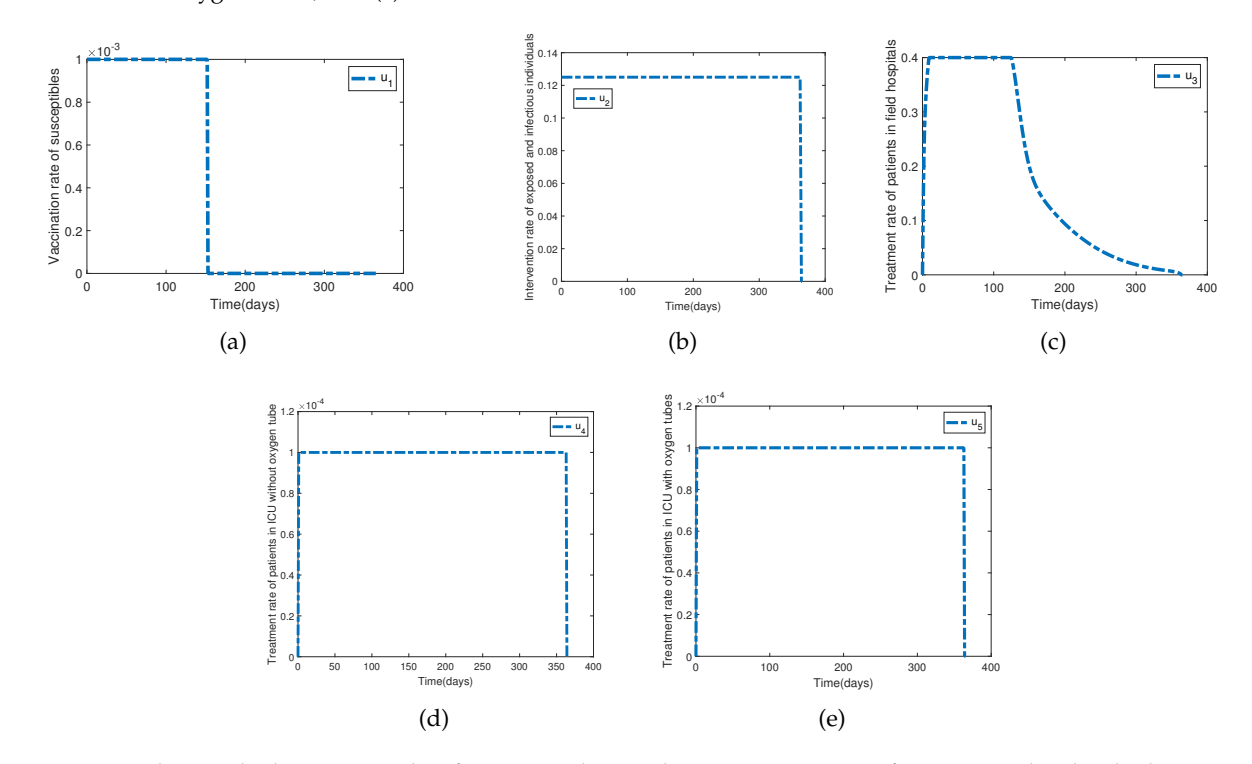


Figure 15: Optimal controls dynamics with a focus on reducing the transmission rate from exposed individuals to susceptible population comprise: (a) vaccination rate  $(u_1(t))$ ; (b) treatment rate of infected individuals in field hospitals  $(u_2(t))$ ; (c) treatment rate of infected individuals in ICU without oxygen tube  $(u_4(t))$ ; and (e) treatment rate of infected individuals in ICU with oxygen tubes  $(u_5(t))$ .

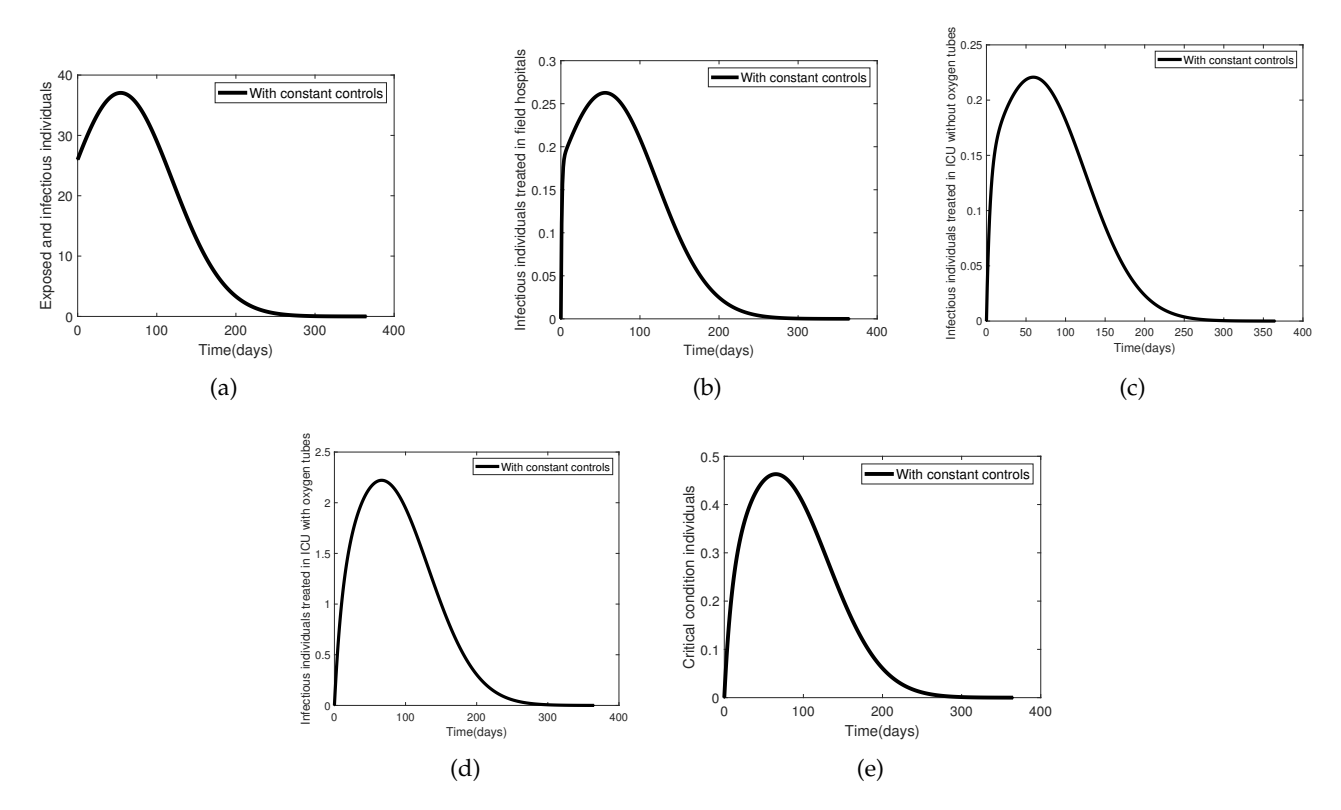


Figure 16: The simulation results of the model cover scenarios involving constant control measures, all aimed at preventing exposed individuals from infecting the susceptible population. These scenarios include (a) exposed and infectious individuals; (b) infectious individuals treated in field hospitals; (c) infectious individuals treated in the ICU without oxygen tubes; (d) infectious individuals treated in the ICU with oxygen tubes; and (e) individuals in critical condition.

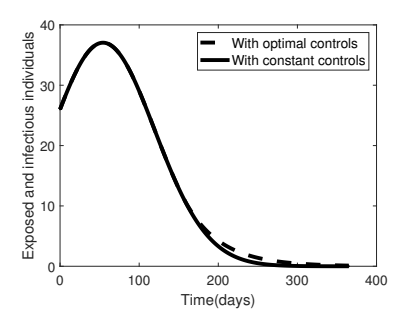


Figure 17: When comparing the constant measures implemented by the Thailand Public Health Administration to optimal control strategies, we observe that the number of new infections for both models remains relatively consistent, with their curves overlapping.

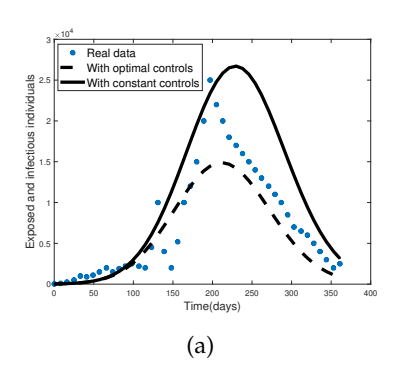
# 8.4. Case study 4: comparing actual control implementations with simulated optimal control

In this section, we will compare the actual control plan implemented by the Thailand Public Health Administration with our simulated optimal control model. During the fourth wave of infections in 2021, Thailand managed to vaccinate about 36.5 percent of the susceptible population, corresponding to a vaccination rate of 0.1 percent of the susceptible population per day. For comparison, in our optimal control scenario, we assume that Thailand could improve slightly, achieving a vaccination rate of 0.11 percent per day, or 40.15 percent by the end of the year.

Figure 18 (a) shows that the total number of new infections in the optimal control model is lower than the actual numbers from Thailand's interventions. Figure 18 (b) depicts that the vaccine should be distributed at a rate of 0.11 percent of the susceptible population per day for the entire year.

Next, we assumed that Thailand could vaccinate the susceptible population at a rate of 0.2 percent per day, or 73 percent by the end of the year. As shown in Figure 19, the infection level becomes very low

under this scenario. Figure 19 (a) shows that the number of new infections per day is significantly lower compared to the actual data, and Figure 19 (b) demonstrates that distributing the vaccine at a daily rate of 0.2 percent of the susceptible population for approximately 230 days (reaching 46 percent in total, without the need to reach 70 percent) can significantly decrease the number of infections to very low levels.



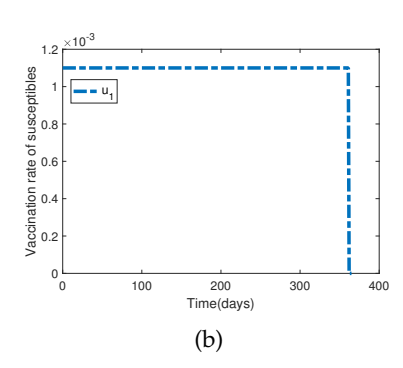
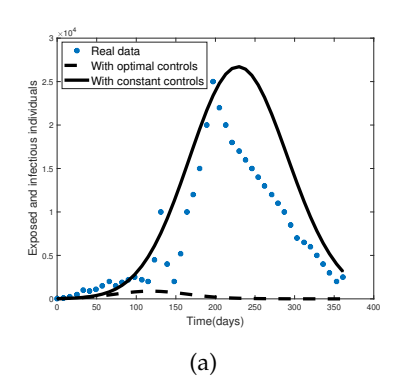


Figure 18: The comparison includes the real data (represented by dots), the simulation results for new exposed and infectious individuals from the initial model (with a vaccination rate of 0.1% per day, referred to as 'with constant controls'), and the optimal control scenario (with a vaccination rate of 0.11% per day, referred to as 'with optimal controls').



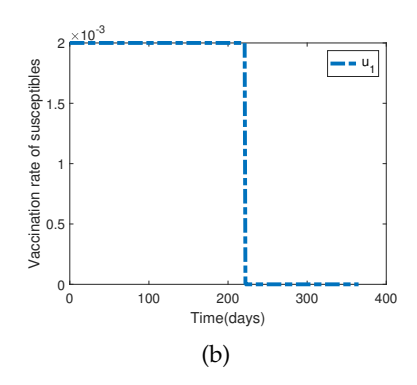


Figure 19: The comparison includes the real data (represented by dots), the simulation results for new exposed and infectious individuals from the initial model (with a vaccination rate of 0.1% per day, referred to as 'with constant controls'), and the optimal control scenario (with a vaccination rate of 0.2% per day, referred to as 'with optimal controls').

#### 9. Conclusion

We have developed a mathematical model using the dataset collected by the Thailand Public Health Administration during the fourth wave of the COVID-19 outbreak in 2021. Both the actual data and the simulation results exhibit similar trends in disease dynamics. Initially, the model incorporated certain constant measures implemented through public intervention programs. However, these measures proved insufficient to halt the spread of the disease at that time. Consequently, we integrated an optimal control study into our model to explore guidelines that could aid in disease control and prove beneficial for future outbreaks.

The model comprises eight differential equations, presenting analytical challenges. We have computed the reproduction number, which, given our parameters, indicates that Thailand faced an  $R_0$  of about 3.03 at the time of the outbreak during the fourth wave. Additionally, this study presents other crucial mathematical insights.

Based on our simulations, the daily vaccination rate of the susceptible population plays a crucial role in controlling the disease. However, if vaccines are limited, additional measures such as wearing masks, social distancing, and washing hands are needed to prevent the susceptible population from getting infected. The simulations also show that if Thailand could vaccinate about 0.2 percent of the susceptible

population daily after the onset of the outbreak, the country would not face such a high number of new infections. With this vaccination rate, the program could conclude in approximately 230 days after the first day of distribution.

Additionally, we investigated the impact of intervention costs and found that higher vaccination costs would prevent the vaccination policy from being sustained for the entire year. In this scenario, other measures would play a crucial role, although they would require a longer time to achieve similar reductions in new infections. Therefore, combining control measures remains essential in effectively controlling the disease.

We acknowledge that our model represents vaccination as a direct shift from the susceptible to the recovered compartment, which simplifies the complex effects of COVID-19 vaccines. This approach was chosen to capture the overall impact of vaccination on reducing infection risk without explicitly modeling disease severity. While it is true that COVID-19 vaccines primarily reduce infection susceptibility, severity, and transmission, our focus was on broad population-level immunity dynamics rather than individual-level clinical outcomes.

That said, incorporating the effect of vaccination on disease severity could provide additional insights. If appropriate and with data available, for our future work, we can extend our model to include a vaccinated-exposed-infected compartment or introduce stratified severity levels among infected individuals. However, we believe our scenario analyses remain informative, as they still capture key epidemiological trends, including the overall reduction in infection rates due to vaccination.

### Appendix A

**Theorem 9.1.** The endemic equilibrium point  $(\varepsilon^*)$  is stable if it satisfies the Routh-Hurwitz criteria where  $I_i^* \geqslant 1$  when i = 1, 2, 3.

*Proof.* We have proved the theorem, and now we show the Routh-Hurwitz criteria as follows:

- (i)  $a_i > 0$ , i = 1, 2, 3, 4, 5;
- (ii)  $a_1 a_2 a_3 > a_3^2 + a_1^2 a_4$ ; and

(iii) 
$$(a_1a_4 - a_5)(a_1a_2a_3 - a_3^2 - a_1^2a_4) > a_5(a_1a_2 - a_3)^2 + a_1a_5^2$$
.

For (i) we want to show that  $a_i > 0$  for i = 1, 2, 3, 4, and 5. Consider that,

$$\begin{split} \alpha_1 &= l_1 + l_2 + l_3 + A_1 + \mu + \varphi_1 - \beta_4 S^* \\ &= l_1 + l_2 + l_3 + A_1 + \mu + \varphi_1 - \beta_4 \frac{l_1}{\beta_1 M_1 + \beta_2 M_2 + \beta_3 M_3 + \beta_4} \\ &= l_1 + l_2 + l_3 + A_1 + \mu + \varphi_1 + l_1 (1 - \frac{\beta_4}{\beta_1 M_1 + \beta_2 M_2 + \beta_3 M_3 + \beta_4}) > 0, \\ \alpha_2 &= l_3 l_4 + l_1 l_3 + l_2 l_3 + + l_1 l_2 + l_1 l_4 + A_1 l_3 + A_1 l_1 + A_1 l_2 \\ &\quad + (\mu + \varphi_1) (l_1 + l_2 + l_3 - \beta_4 S^*) - \beta_3 \alpha_3 - \beta_4 S^* l_4 - \beta_2 \alpha_2 - \beta_4 S^* l_3 - \beta_4 S^* l_2 - \alpha_1 \beta_1. \end{split}$$

For  $a_2$ , we see that

$$\begin{split} l_1 - \beta_4 S^* &= (1 - \frac{\beta_4}{\beta_1 M_1 + \beta_2 M_2 + \beta_3 M_3 + \beta_4}) l_1 > 0, \\ A_1 l_1 - \beta_3 \alpha_3 > \beta_3 * I_3^* \alpha_3 - \beta_3 \alpha_3 &= (I_3^* - 1) \beta_3 \alpha_3 > 0, \\ A_1 l_1 - \beta_1 \alpha_1 > \beta_1 * I_1^* \alpha_1 - \beta_1 \alpha_1 &= (I_1^* - 1) \beta_1 \alpha_1 > 0, \\ A_1 l_1 - \beta_2 \alpha_2 > \beta_2 * I_2^* \alpha_2 - \beta_2 \alpha_2 &= (I_2^* - 1) \beta_2 \alpha_2 > 0, \\ l_1 l_4 - \beta_4 S^* l_4 &= (l_1 - \beta_4 S^*) l_4 \\ &= (l_1 - \beta_4 \frac{l_1}{\beta_1 M_1 + \beta_2 M_2 + \beta_3 M_3 + \beta_4}) l_4 \end{split}$$

$$=(1-\frac{\beta_4}{\beta_1M_1+\beta_2M_2+\beta_3M_3+\beta_4})l_1l_4>0,\\ l_1l_3-\beta_4S^*l_3=(l_1-\beta_4S^*)l_3>0,\\ l_1l_2-\beta_4S^*l_2=(l_1-\beta_4S^*)l_2>0.$$

Thus  $a_2 > 0$ . Next, we will show that  $a_3 > 0$ . We have that

$$\begin{split} \alpha_3 &= l_1 l_2 l_3 + l_1 l_3 l_4 + l_2 l_3 l_4 + l_1 l_2 l_4 + A_1 l_3 l_4 + A_1 l_1 l_3 + A_1 l_2 l_3 + A_1 l_1 l_2 + A_1 l_1 l_4 - \beta_3 \alpha_3 l_3 - \beta_3 \alpha_1 h_2 - \beta_3 \alpha_3 l_2 \\ &- \beta_3 \alpha_2 \lambda_1 - \beta_2 \alpha_2 l_4 - \beta_4 S^* l_3 l_4 - \beta_4 S^* l_2 l_3 - \alpha_1 \beta_1 l_4 - \beta_2 \alpha_1 h_1 - \beta_2 \alpha_2 l_2 - \beta_4 S^* l_2 l_3 \\ &- \beta_1 \alpha_1 l_3 + (l_1 l_4 + l_1 l_3 + l_2 l_3 + l_1 l_2 - \beta_3 \alpha_3 - \beta_4 S^* l_4 - \beta_2 \alpha_2 - \beta_4 S^* l_3 - \beta_4 S^* l_2 - \alpha_1 \beta_1) (\mu + \varphi_1), \end{split}$$

and

$$\begin{split} A_1l_1l_2 - \beta_3\alpha_1h_2 &> \beta_3I_3^*\alpha_1h_2 - \beta_3\alpha_1h_2 = (I_3^*-1)\beta_3\alpha_1h_2 > 0, \\ A_1l_1l_2 - \beta_2\alpha_1h_1 &> \beta_2I_3^*\alpha_1h_1 - \beta_2\alpha_1h_1 > 0, \\ A_1l_1l_3 - \beta_3\alpha_2\lambda_1 &> \beta_3I_3^*\alpha_2\lambda_1 - \beta_3\alpha_2\lambda_1 > 0, \\ A_1l_1l_3 - \beta_3\alpha_3l_3 &> \beta_3I_3^*\alpha_3l_3 - \beta_3\alpha_3l_3 > 0, \\ A_1l_1l_2 - \beta_3\alpha_3l_2 &> \beta_3I_3^*\alpha_3l_2 - \beta_3\alpha_3l_2 > 0, \\ A_1l_1l_4 - \beta_2\alpha_2l_4 &> \beta_2I_2^*\alpha_2l_4 - \beta_2\alpha_2l_4 > 0, \\ l_1l_3l_4 - \beta_4S^*l_3l_4 &= (l_1 - \beta_4S^*)l_3l_4 > 0, \\ l_1l_2l_3 - \beta_4S^*l_2l_3 &= (l_1 - \beta_4S^*)l_2l_3 > 0, \\ A_1l_1l_4 - \alpha_1\beta_1l_4 &> \beta_1I_1^*\alpha_1l_4 - \alpha_1\beta_1l_4 > 0, \\ A_1l_1l_2 - \beta_2\alpha_2l_2 &> \beta_1I_1^*\alpha_2l_2 - \beta_2\alpha_2l_2 > 0, \\ l_1l_2l_3 - \beta_4S^*l_2l_3 &> (l_1 - \beta_4S^*)l_2l_3 > 0, \\ A_1l_1l_3 - \beta_1\alpha_1l_3 &> \beta_1I_1^*\alpha_1l_3 - \beta_1\alpha_1l_3 > 0, \\ A_1l_1l_3 - \beta_2\alpha_2(\mu + \phi_1) &> (I_2^*-1)\beta_2\alpha_2(\mu + \phi_1) > 0, \\ A_1l_1l_4 - \beta_3\alpha_3(\mu + \phi_1) &> (I_1^*-1)\beta_1\alpha_1(\mu + \phi_1) > 0, \\ A_1l_2 - \beta_1\alpha_1(\mu + \phi_1) &> (I_1^*-1)\beta_1\alpha_1(\mu + \phi_1) > 0, \\ l_1l_3 - \beta_4S^*l_4 &= (l_1 - \beta_4S^*)l_4 > 0, \\ l_1l_3 - \beta_4S^*l_3 &= (l_1 - \beta_4S^*)l_3 > 0, \\ l_1l_2 - \beta_4S^*l_2 &= (l_1 - \beta_4S^*)l_2 > 0. \end{split}$$

Thus  $a_3 > 0$ . Next, we show that  $a_4 > 0$ . Consider that we have

$$\begin{split} \alpha_4 &= l_1 l_2 l_3 l_4 + A_1 l_1 l_3 l_4 + A_1 l_2 l_3 l_4 + A_1 l_1 l_2 l_4 + A_1 l_1 l_2 l_3 - \beta_3 \alpha_1 h_2 l_3 - \beta_3 \alpha_3 l_2 l_3 \\ &- \beta_3 \alpha_1 h_1 \lambda_1 - \beta_3 \alpha_2 l_2 \lambda_1 - \beta_2 \alpha_1 h_1 l_4 - \beta_2 \alpha_2 l_2 l_4 - \beta_4 S^* l_2 l_3 l_4 - \alpha_1 \beta_1 l_3 l_4 \\ &+ (\mu + \varphi_1) (l_1 l_3 l_4 + l_2 l_3 l_4 + l_1 l_2 l_4 + l_1 l_2 l_3 - \beta_3 \alpha_3 l_3 - \beta_3 \alpha_1 h_2 - \beta_3 \alpha_3 l_2 - \beta_3 \alpha_2 \lambda_1 \\ &- \beta_2 \alpha_2 l_4 - \beta_4 S^* l_3 l_4 - \beta_4 S^* l_2 l_3 - \alpha_1 \beta_1 l_4 - \beta_2 \alpha_1 h_1 - \beta_2 \alpha_2 l_2 - \beta_4 S^* l_2 l_4 - \alpha_1 \beta_1 l_3), \end{split}$$

and

$$\begin{split} &l_1l_3l_4-\beta_4S^*l_3l_4=(1-\frac{\beta_4}{\beta_1M_1+\beta_2M_2+\beta_3M_3+\beta_4})l_1l_2l_3>0,\\ &l_1l_2l_3-\beta_4S^*l_2l_3=(1-\frac{\beta_4}{\beta_1M_1+\beta_2M_2+\beta_3M_3+\beta_4})l_1l_2l_3>0,\\ &l_1l_2l_4-\beta_4S^*l_2l_4=(1-\frac{\beta_4}{\beta_1M_1+\beta_2M_2+\beta_3M_3+\beta_4})l_1l_2l_4>0, \end{split}$$

$$\begin{split} &A_1l_1l_2l_3 - \beta_3\alpha_1h_2l_3 > \beta_3I_3^*\alpha_1h_2l_3 - \beta_3\alpha_1h_2l_3 = (I_3^*-1)\beta_3\alpha_1h_2l_3 > 0, \\ &A_1l_1l_2l_3 - \beta_3\alpha_3l_2l_3 > \beta_3I_3^*\alpha_3l_2l_3 - \beta_3\alpha_3l_2l_3 > 0, \\ &A_1l_1l_3 - \beta_3\alpha_1h_1\lambda_1 > \beta_3I_3^*\alpha_1h_1\lambda_1 - \beta_3\alpha_1h_1\lambda_1 > 0, \\ &A_1l_1l_3 - \beta_3\alpha_2l_2\lambda_1 > \beta_3I_3^*\alpha_2l_2\lambda_1 - \beta_3\alpha_2l_2l_1 > 0, \\ &A_1l_1l_2l_4 - \beta_2\alpha_1h_1l_4 > \beta_2I_2^*\alpha_1h_1l_4 - \beta_2\alpha_1h_1l_4 > 0, \\ &A_1l_1l_2l_4 - \beta_2\alpha_2l_2l_4 < \beta_2I_2^*\alpha_2l_2l_4 - \beta_2\alpha_2l_2l_4 > 0, \\ &l_1l_2l_3l_4 - \beta_4S^*l_2l_3l_4 = (1 - \frac{\beta_4}{\beta_1M_1 + \beta_2M_2 + \beta_3M_3 + \beta_4})l_1l_2l_3l_4 > 0, \\ &A_1l_1l_3l_4 - \alpha_1\beta_1l_3l_4 > \alpha_1\beta_1I_1^*l_3l_4 - \alpha_1\beta_1l_3l_4 > 0, \\ &A_1l_1l_3l_4 - \beta_3\alpha_3l_3 > \beta_3I_3^*\alpha_3l_3l_4 - \beta_3\alpha_3l_3(\mu + \varphi_1) > \beta_3\alpha_3l_3(\mu + \varphi_1)(I_3^*-1) > 0, \\ &A_1l_1l_2l_4 - \beta_3\alpha_3l_2 > \beta_3\alpha_3l_2(\mu + \varphi_1)(I_3^*-1) > 0, \\ &A_1l_1l_2l_4 - \beta_3\alpha_2\lambda_1 > \beta_3I_3^*\alpha_2\lambda_1l_4 - \beta_3\alpha_2\lambda_1(\mu + \varphi_1) > 0, \\ &A_1l_1l_2l_4 - \beta_2\alpha_2l_4 > \beta_2I_2^*\alpha_2l_2l_4 - \beta_2\alpha_2l_4(\mu + \varphi_1) > 0, \\ &A_1l_1l_2l_4 - \alpha_1\beta_1l_4 > \beta_1I_1^*\alpha_1l_2l_4 - \alpha_1\beta_1l_4(\mu + \varphi_1) > 0, \\ &A_1l_1l_2l_4 - \beta_2\alpha_2h_1 > \beta_2I_2^*\alpha_2h_1l_4 - \beta_2\alpha_2h_1(\mu + \varphi_1) > 0, \\ &A_1l_1l_2l_4 - \beta_2\alpha_2l_2 > \beta_2I_2^*\alpha_2l_2l_4 - \beta_2\alpha_2l_2(\mu + \varphi_1) > 0, \\ &A_1l_1l_2l_4 - \beta_2\alpha_2l_2 > \beta_2I_2^*\alpha_2l_2l_4 - \beta_2\alpha_2l_2(\mu + \varphi_1) > 0, \\ &A_1l_1l_2l_4 - \beta_2\alpha_2l_2 > \beta_2I_2^*\alpha_2l_2l_4 - \beta_2\alpha_2l_2(\mu + \varphi_1) > 0, \\ &A_1l_1l_2l_4 - \beta_2\alpha_2l_2 > \beta_2I_2^*\alpha_2l_2l_4 - \beta_2\alpha_2l_2(\mu + \varphi_1) > 0, \\ &A_1l_1l_2l_4 - \beta_2\alpha_2l_2 > \beta_2I_2^*\alpha_2l_2l_4 - \beta_2\alpha_2l_2(\mu + \varphi_1) > 0, \\ &A_1l_1l_2l_4 - \beta_2\alpha_2l_2 > \beta_2I_2^*\alpha_2l_2l_4 - \beta_2\alpha_2l_2(\mu + \varphi_1) > 0, \\ &A_1l_1l_2l_4 - \beta_2\alpha_2l_2 > \beta_2I_2^*\alpha_2l_2l_4 - \beta_2\alpha_2l_2(\mu + \varphi_1) > 0, \\ &A_1l_1l_3l_4 - \alpha_1\beta_1l_3 > \alpha_1\beta_1I_1^*l_3l_4 - \alpha_1\beta_1l_3(\mu + \varphi_1) > 0. \end{split}$$

Thus  $a_4 > 0$ . Now we check  $a_5 > 0$ . Consider that

$$\begin{split} a_5 &= A_1 l_1 l_2 l_3 l_4 + (l_1 l_2 l_3 l_4 - \beta_3 \alpha_1 h_2 l_3 - \beta_3 \alpha_3 l_2 l_3 - \beta_3 \alpha_1 h_1 \lambda_1 - \beta_3 \alpha_2 l_2 \lambda_1 \\ &- \beta_2 \alpha_1 h_1 l_4 - \beta_2 \alpha_2 l_2 l_4 - \beta_4 S^* l_2 l_3 l_4 - \beta_1 \alpha_1 l_3 l_4) (\mu + \varphi_1), \end{split}$$

and similar to  $a_4$ , we have

$$\begin{split} A_1 l_1 l_2 l_3 l_4 - (\beta_3 \alpha_1 h_2 l_3 + \beta_3 \alpha_3 l_2 l_3 + \beta_3 \alpha_1 h_1 \lambda_1 + \beta_3 \alpha_2 l_2 \lambda_1) (\mu + \varphi_1) &> 0, \\ A_1 l_1 l_2 l_3 l_4 - (\beta_2 \alpha_1 h_1 l_4 + \beta_2 \alpha_2 l_2 l_4) (\mu + \varphi_1) &> 0, \end{split}$$

and

$$A_1l_1l_2l_3l_4 - \beta_1\alpha_1l_3l_4(\mu + \phi_1) > 0.$$

Next, consider that

$$\begin{split} l_1 l_2 l_3 l_4 - \beta_4 S^* l_2 l_3 l_4 &= l_1 l_2 l_3 l_4 - \frac{\beta_4 l_1}{\beta_1 M_1 \beta_2 M_2 \beta_3 M_3 + \beta_4} l_2 l_3 l_4 \\ &= (1 - \frac{\beta_4}{\beta_1 M_1 \beta_2 M_2 + \beta_3 M_3 + \beta_4}) l_1 l_2 l_3 l_4 > 0. \end{split}$$

Thus  $a_5 > 0$ . For the second criteria, we have to show that  $a_1 a_2 a_3 > a_3^2 + a_1^2 a_4$ , or  $a_1 a_2 a_3 - a_3^2 - a_1^2 a_4 > 0$ . After some algebraic manipulations, we have that

$$\begin{split} &-l_2 l_3 A_1 - l_1 l_2 l_4 - l_1 l_3 l_4 - l_2 l_3 l_4 - l_3 A_1 l_4 + l_3 l_4 \alpha_1 + l_2 \beta_2 \alpha_2 l_2 \beta_3 \alpha_3 + l_3 \beta_3 \alpha_3 \\ &+ l_4 \beta_1 \alpha_1 + l_4 \beta_2 \alpha_2 + \beta_2 h_1 \alpha_1 + \beta_3 \alpha_1 h_2 + \beta_3 \alpha_2 \lambda_1 + 2 l_2 l_3 \beta_4 S^* + l_3 \beta_4 S^* l_4)^2, \end{split}$$

and

$$\begin{split} l_1 l_3 l_4 - l_3 \beta_4 S^* l_4 &= (1 - \frac{\beta_4}{\beta_1 M_1 + \beta_2 M_2 + \beta_3 M_3 + \beta_4}) l_1 l_3 l_4 > 0, \\ l_1 l_2 l_3 l_4 - l_2 l_3 \beta_4 S^* l_4 &= (1 - \frac{\beta_4}{\beta_1 M_1 + \beta_2 M_2 + \beta_3 M_3 + \beta_4}) l_1 l_2 l_3 l_4 > 0, \\ l_1 l_2 l_3 - l_2 l_3 \beta_4 S^* &= (1 - \frac{\beta_4}{\beta_1 M_1 + \beta_2 M_2 + \beta_3 M_3 + \beta_4}) l_1 l_2 l_3 > 0, \\ l_2 l_3 A_1 l_4 - l_2 l_3 \beta_3 l_4 > (I_3^* - 1) \beta_3 l_2 l_3 l_4 > 0, \\ l_1 l_3 A_1 l_4 - l_3 l_4 \beta_1 \alpha_1 > (I_1^* - 1) \beta_1 \alpha_1 l_3 l_4 > 0, \\ l_1 l_2 A_1 l_4 - l_4 \beta_2 h_1 \alpha_1 > (I_1^* - 1) \beta_2 l_4 h_1 \alpha_1 > 0, \\ l_1 l_2 l_3 l_4 - l_2 l_3 \beta_4 S^* l_4 &= (1 - \frac{\beta_4}{\beta_1 M_1 + \beta_2 M_2 + \beta_3 M_3 + \beta_4}) l_1 l_2 l_3 l_4 > 0. \end{split}$$

Hence,  $a_1a_2a_3 - a_3^2 - a_1^2a_4 > 0$ , that is  $a_1a_2a_3 > a_3^2 + a_1^2a_4$ , and now the second criteria holds. Next, we will show that  $(a_1a_4 - a_5)(a_1a_2a_3 - a_3^2 - a_1^2a_4) > a_5(a_1a_2 - a_3)^2 + a_1a_5^2$ . First, from the second criteria we have  $a_1a_2a_3 > a_3^2 + a_1^2a_4$ . Then  $a_1a_2a_3 - a_3^2 - a_1^2a_4 > 0$ , or  $a_1a_2 - a_3 > \frac{a_1^2a_4}{a_3}$ , and from

$$(a_1a_4 - a_5)(a_1a_2a_3 - a_3^2 - a_1^2a_4) > 0,$$

with  $a_5(a_1a_2-a_3)^2+a_1a_5^2>0$ , then we have  $a_1a_4-a_5>0$ , and so  $a_1a_4>a_5$ . Therefore,

$$a_5(a_1a_2-a_3)^2+a_1a_5^2>a_5\frac{(a_1^2a_4)^2}{a_3^2}+a_1a_5^2>a_1a_5^2(\frac{a_1a_5}{a_3^2}+1)>\frac{a_1^2a_5^3}{a_3^2}.$$

Thus

$$(a_1a_4 - a_5)(a_1a_2a_3 - a_3^2 - a_1^2a_4) > \frac{a_1^2a_5^3}{a_2^2},$$

or

$$\alpha_3^2(\alpha_1\alpha_4-\alpha_5)(\alpha_1\alpha_2\alpha_3-\alpha_3^2-\alpha_1^2-\alpha_1^2\alpha_4)>\alpha_1^2\alpha_5^3.$$

We only need to show that  $a_3^2(\alpha_1\alpha_4-\alpha_5)(\alpha_1\alpha_2\alpha_3-\alpha_3^2-\alpha_1^2-\alpha_1^2\alpha_4)-\alpha_1^2\alpha_5^3>0$ . With some algebraic manipulations, we have that

$$\begin{split} a_3^2(\alpha_1\alpha_4-\alpha_5)(\alpha_1\alpha_2\alpha_3-\alpha_3^2-\alpha_1^2-\alpha_1^2\alpha_4) - a_1^2\alpha_5^3 \\ &= (l_1+l_2+l_3+A_1+\mu+\varphi_1-\beta_4S^*)((\mu+\varphi_1)(\beta_1\alpha_1-l_1l_3-l_2l_3-l_3l_4\\ &+\beta_2\alpha_2+\beta_3\alpha_3+l_2\beta_4S^*+l_3\beta_4S^*+\beta_4S^*l_4) - l_1l_2A_1-l_1l_3A_1-l_2l_3A_1\\ &-l_1l_2l_4-l_1l_3l_4-l_2l_3l_4-l_3A_1l_4+l_3\beta_1\alpha_1+l_2\beta_2\alpha_2+l_2\beta_3\alpha_3\\ &+l_3\beta_3\alpha_3+l_4\beta_1\alpha_1+l_4\beta_2\alpha_2+\beta_2h_1\alpha_1+\beta_3\alpha_1h_2+\beta_3\alpha_2\lambda_1+2l_2l_3\beta_4S^*\\ &+l_3\beta_4S^*l_4)^2+((\mu+\varphi_1)(l_2l_3\beta_3\alpha_3+l_3l_4\beta_1\alpha_1+l_2l_4\beta_2\alpha_2+l_2\beta_3\alpha_2\lambda_1\\ &+l_4\beta_2h_1\alpha_1+l_3\beta_3\alpha_1h_2+\beta_3h_1\alpha_1\lambda_1-l_1l_2l_3l_4+l_2l_3\beta_4S^*l_4)-l_1l_2l_3A_1l_4)^2\\ &\times(l_1+l_2+l_3+A_1+\mu+\varphi_1-\beta_4S^*)^2+((\mu+\varphi_1)(\beta_1\alpha_1-l_1l_3-l_2l_3-l_3l_4-l_1l_2+\beta_2\alpha_2+l_4\beta_2h_1\alpha_1+l_3\beta_3\alpha_1h_2+\beta_3h_1\alpha_1\lambda_1+l_1l_2l_3l_4-l_2l_3\beta_4S^*l_4) \end{split}$$

$$\begin{split} &+l_2l_2l_3A_1l_4)(l_1+l_2+l_3+A_1+\mu+\varphi_1-\beta_4S^*)((\mu+\varphi_1)\\ &\times(\beta_1\alpha_1+l_1l_3+l_2l_3+l_3l_4+l_1l_2+l_1l_4+\beta_2\alpha_2+\beta_3\alpha_3-l_2\beta_4S^*-l_3\beta_4S^*\\ &-\beta_4S^*l_4)+l_1l_2A_1+l_1l_3A_1+l_2l_3A_1-l_1l_2l_4-l_1l_3l_4-l_2l_3l_4+l_3A_1l_4\\ &+l_1A_1l_4+l_3\beta_1\alpha_1+l_2\beta_2\alpha_2-l_2\beta_3\alpha_3-l_3\beta_3\alpha_3-l_4\beta_1\alpha_1-l_4\beta_2\alpha_2\\ &-\beta_2h_1\alpha_1-\beta_3\alpha_1h_2-\beta_3\alpha_2\lambda_1+2l_2l_3\beta_4S^*+l_3\beta_4S^*l_4). \end{split}$$

Next, we have that

$$\begin{split} l_1 l_2 l_3 l_4 - l_2 l_3 \beta_4 S^* l_4 &= (1 - \frac{\beta_4}{1 - \beta_1 M_1 + \beta_2 M_2 + \beta_3 M_3 + \beta_4}) l_1 l_2 l_3 l_4 > 0, \\ l_1 A_1 l_4 - l_4 \beta_1 \alpha_1 &> (I_1^* - 1) \alpha_1 l_4 \beta_1 > 0, \\ l_1 l_2 A_1 - \beta_2 h_1 \alpha_1 &> (I_2^* - 1) \alpha_1 h_1 \beta_2 > 0, \\ l_1 l_3 A_1 - \beta_3 \alpha_2 \lambda_1 &> (I_3^* - 1) \alpha_2 \lambda_1 \beta_3 > 0, \\ l_1 l_2 A_1 - \beta_3 \alpha_1 h_2 &> (I_3^* - 1) \alpha_1 h_2 \beta_3 > 0, \\ l_1 l_2 A_1 - l_2 \beta_3 \alpha_3 &> (I_3^* - 1) l_2 \alpha_3 \beta_3 > 0, \\ l_1 l_3 A_1 - l_3 \beta_3 \alpha_3 &> (I_3^* - 1) \alpha_3 \beta_3 l_3 > 0, \\ l_1 l_4 - l_4 \beta_2 \alpha_2 &> (I_2^* - 1) \beta_2 l_4 \alpha_2 > 0. \end{split}$$

Thus the last criteria holds, that is,  $(a_1a_4-a_5)(a_1a_2a_3-a_3^2-a_1^2a_4)>a_5(a_1a_2-a_3)^2+a_1a_5^2$ . We have also computed these criteria and found that they are all satisfied, with values  $a_1=1.0237,\ a_2=0.1791,\ a_3=0.0215,\ a_4=0.0023,\ a_5=2.3849\times 10^{-6},\ a_1a_2a_3-a_3^2-a_1^2a_4=0.0011>0,\ and\ (a_1a_4-a_5)(a_1a_2a_3-a_3^3-a_1^2a_4)-a_5(a_1a_2-a_3)^2-a_1a_5^2=3.4989\times 10^{-6}>0.$ 

#### Appendix B

From our model, we have

$$\mathcal{F} = \left[ \begin{array}{c} \left(\beta_1 I_1 + \beta_2 I_2 + \beta_3 I_3 + \beta_4 E\right) S \\ 0 \\ 0 \\ 0 \\ 0 \end{array} \right] \quad \text{and} \quad \mathcal{V} = \left[ \begin{array}{c} (\alpha_1 + \alpha_2 + \alpha_3 + \alpha_4 + \mu + \gamma_5 + \varphi_2) E \\ (\mu + d_1 + \gamma_1 + h_1 + h_2 + h_3 + \varphi_3) I_1 - \alpha_1 E \\ (\mu + d_2 + \gamma_2 + \lambda_1 + \lambda_2 + \varphi_4) I_2 - \alpha_2 E - h_1 I_1 \\ (\mu + d_3 + \gamma_3 + \epsilon + \varphi_5) I_3 - \alpha_3 E - h_2 I_1 - \lambda_1 I_2 \\ (\mu + d_4 + \gamma_4) I_4 - \alpha_4 E - h_3 I_1 - \lambda_2 I_2 - \epsilon I_3 \end{array} \right] .$$

Next, we find F and V by calculating the Jacobian of  $\mathcal{F}$  and  $\mathcal{V}$ , respectively, then substituting  $\epsilon_0 = \left(\frac{\Lambda}{\mu + \Phi_1}, 0, 0, 0, 0, 0, \frac{\Phi_1 \Lambda}{\mu (\mu + \Phi_1)}, 0\right)$  into the Jacobian matrices F and V, we have

where  $l_1 = \alpha_1 + \alpha_2 + \alpha_3 + \alpha_4 + \mu + \gamma_5 + \phi_2$ ,  $l_2 = \mu + d_1 + \gamma_1 + h_1 + h_2 + h_3 + \phi_3$ ,  $l_3 = \mu + d_2 + \gamma_2 + \lambda_1 + \lambda_2 + \phi_4$ ,  $l_4 = \mu + d_3 + \gamma_3 + \epsilon + \phi_5$ , and  $l_5 = \mu + d_4 + \gamma_4$ . It follows that

$$V^{-1}(\varepsilon_0) = \begin{bmatrix} \frac{\frac{1}{l_1}}{\frac{1}{l_1 l_2}} \\ \frac{\alpha_1 h_1 + \alpha_2 l_2}{l_1 l_2 l_3} \\ \frac{\alpha_3 l_2 + \alpha_1 h_2}{l_1 l_2 l_4} + \frac{\alpha_1 h_1 \lambda_1 + \alpha_2 \lambda_1 l_2}{l_1 l_2 l_3 l_4} \\ \frac{\alpha_1 h_1 \lambda_1 \varepsilon + \alpha_1 h_3 l_3 l_4 + \alpha_1 h_1 \lambda_2 l_4 + \varepsilon \alpha_1 h_2 l_3 + \varepsilon \alpha_2 \lambda_2 l_2 + \alpha_4 l_2 l_3 l_4 + \alpha_2 \lambda_2 l_2 l_4 + \varepsilon \alpha_2 l_2 l_3}{l_1 l_2 l_3 l_4 l_5} \end{bmatrix}$$

$$\begin{bmatrix} 0 & 0 & 0 & 0 \\ \frac{1}{l_2} & 0 & 0 & 0 \\ 0 & \frac{1}{l_3} & 0 & 0 \\ \frac{\lambda_1 h_1 + h_2 l_3}{l_2 l_3 l_4} & \frac{\lambda_1}{l_3 l_4} & \frac{1}{l_4} & 0 \\ \frac{\epsilon l_1 h_1 \lambda_1 + h_3 l_1 l_3 l_4 + \lambda_2 l_1 l_3 l_4 + \epsilon h_2 l_1 l_3}{l_1 l_2 l_3 l_4 l_5} & \frac{\epsilon \lambda_1 + \lambda_2 l_4}{l_3 l_4 l_5} & \frac{\epsilon}{l_4 l_5} & \frac{1}{l_5} \end{bmatrix}.$$

Next, we find the eigenvalues of the Jacobian matrix by considering solving  $det(FV^{-1} - \lambda I) = 0$ . Thus,  $R_0$  is the spectral radius of  $FV^{-1}$ , therefore we then obtain the basic reproduction number  $(\mathcal{R}_0)$ , which yields

$$\begin{split} \mathcal{R}_0 &= \left[ \frac{\Lambda}{(\mu + \varphi_1)(\alpha_1 + \alpha_2 + \alpha_3 + \alpha_4 + \mu + \gamma_5 + \varphi_2)} \right] \left[ \beta_4 + \frac{\alpha_1\beta_1}{\mu + d_1 + \gamma_1 + h_1 + h_2 + h_3 + \varphi_3} \right. \\ &\quad + \frac{\alpha_1\beta_2h_2 + \alpha_3\beta_2(\mu + d_1 + \gamma_1 + h_1 + h_2 + h_3 + \varphi_3)}{\left( \mu + d_1 + \gamma_1 + h_1 + h_2 + h_3 + \varphi_3 \right) \left( \mu + d_2 + \gamma_2 + \lambda_1 + \lambda_2 + \varphi_4 \right)} \\ &\quad + \frac{\alpha_1\beta_3h_2 + \alpha_3\beta_3(\mu + d_1 + \gamma_1 + h_1 + h_2 + h_3 + \varphi_3)}{\left( \mu + d_1 + \gamma_1 + h_1 + h_2 + h_3 + \varphi_3 \right) \left( \mu + d_3 + \gamma_3 + \epsilon + \varphi_5 \right)} \\ &\quad + \frac{\alpha_1\beta_3h_1\lambda_1 + \alpha_1\lambda_2(\mu + d_1 + \gamma_1 + h_1 + h_2 + h_3 + \varphi_3)}{\left( \mu + d_1 + \gamma_1 + h_1 + h_2 + h_3 + \varphi_3 \right) \left( \mu + d_2 + \gamma_2 + \lambda_1 + \lambda_2 + \varphi_4 \right) \left( \mu + d_3 + \gamma_3 + \epsilon + \varphi_5 \right)} \\ &\quad = \frac{\Lambda\left(\beta_4\ell_2\ell_3\ell_4 + \alpha_1\beta_1\ell_3\ell_4 + \beta_2\left(\alpha_1h_1 + \alpha_2\ell_2\right)\ell_4 + \beta_3\left(\alpha_3\ell_2\ell_3 + \alpha_1h_2\ell_3 + \alpha_1h_1\lambda_1 + \alpha_2\lambda_1\ell_2\right)\right)}{(\mu + \varphi_1)\ell_1\ell_2\ell_3\ell_4}, \end{split}$$

where

$$\begin{split} \ell_1 &= \alpha_1 + \alpha_2 + \alpha_3 + \alpha_4 + \mu + \gamma_5 + \varphi_2, \\ \ell_3 &= \mu + d_2 + \gamma_2 + \lambda_1 + \lambda_2 + \varphi_4, \end{split} \qquad \begin{aligned} \ell_2 &= \mu + d_1 + \gamma_1 + h_1 + h_2 + h_3 + \varphi_3, \\ \ell_4 &= \mu + d_3 + \gamma_3 + \epsilon + \varphi_5. \end{aligned}$$

#### Acknowledgment

This work was supported by Naresuan University (NU), and National Science, Research and Innovation Fund (NSRF), Grant NO. R2567B016.

# Declaration of generative AI and AI-assisted technologies in the writing process

During the preparation of this work the author(s) used ChatGPT in order to improve readability and language. After using this tool/service, the author(s) reviewed and edited the content as needed and take(s) full responsibility for the content of the publication.

#### References

- [1] M. Aakash, C. Gunasundari, Effect of partially and fully vaccinated individuals in some regions of India: A mathematical study on COVID-19 outbreak, Commun. Math. Biol. Neurosci., 2023 (2023), 25 pages. 1
- [2] M. Aakash, C. Gunasundari, S. Sabarinathan, S. M. Boulaaras, A. Himadan, *Mathematical insights into the SEIQRD model with Allee and fear dynamics in the context of COVID-19*, Partial Differ. Equ. Appl. Math., **11** (2024).
- [3] M. O. Adewole, A. A. Onifade, F. A. Abdullah, F. Kasali, A. I. M. Ismail, *Modeling the dynamics of COVID-19 in Nigeria*, Int. J. Appl. Comput. Math., 7 (2021), 1–67.
- [4] I. Ahmed, G. U. Modu, A. Yusuf, P. Kumam, I. Yusuf, A mathematical model of coronavirus disease (COVID-19) containing asymptotic and symptomatic classes, Results Phys., 21 (2021), 14 pages.
- [5] T. Carbollo, I. Bouzalmat, A. Settati, A. Lahrouz, A. N. Brahim, B. Harchaoui, Stochastic COVID-19 epidemic model incorporating asymptomatic and isolated compartments, Math. Methods Appl. Sci., 48 (2025), 8400–8422.

- [6] C. Castillo-Chavez, Z. Feng, W. Huang, *On the computation of* R<sub>0</sub> *and its role on global stability*, In: Mathematical approaches for emerging and reemerging infectious diseases: an introduction (Minneapolis, MN, 1999), Springer, New York, (2002). 5
- [7] N. Chitnis, J. M. Hyman, J. M. Cushing, Determining important parameters in the spread of malaria through the sensitivity analysis of a mathematical model, Bull. Math. Biol., 70 (2008), 1272–1296. 4
- [8] Corona Virus Disease Situation in Thailand, Department of Disease Control, Ministry of Public Health, Thailand (access 27 September 2024). 1, 8
- [9] Corona Virus Thailand, Worldometer (accessed 27 September 2024). 1, 2
- [10] COVID-19 Thailand, World Health Organization (WHO) (accessed 27 September 2024). 1, 8, 2, 5
- [11] I. Darti, Trisilowati, M. Rayungsari, R. R. Musafir, A. Suryanto, A SEIQRD epidemic model to study the dynamics of COVID-19 disease, Commun. Math. Biol. Neurosci., 2023 (2023), 19 pages. 1
- [12] P. Das, R. K. Upadhyay, A. K. Misra, F. A. Rihan, D. Ghosh, *Mathematical model of COVID-19 with comorbidity and controlling using non-pharmaceutical interventions and vaccination*, Nonlinear Dyn., **106** (2021), 1213–1227.
- [13] B. Dhar, P. K. Gupta, M. Sajid, Solution of a dynamical memory effect COVID-19 infection system with leaky vaccination efficacy by non-singular kernel fractional derivatives, Math. Biosci. Eng., 19 (2022), 4341–4367.
- [14] J. K. Ghosh, S. K. Biswas, S. Sarkar, U. Ghosh, Mathematical modelling of COVID-19: A case study of Italy, Math. Comput. Simul., 194 (2022), 1–18. 2
- [15] M. Gümüş, K. Türk, A note on the dynamics of a COVID-19 epidemic model with saturated incidence rate, Eur. Phys. J. Spec. Top., 234 (2024), 1751–1758. 1
- [16] I. M. Hezam, A. Foul, A. Alrasheedi, *A dynamic optimal control model for COVID-19 and cholera co-infection in Yemen*, Adv. Differ. Equ., **2021** (2021), 30 pages.
- [17] J. I. Irunde, J. Z. Ndendya, J. A. Mwasunda, P. K. Robert, Modeling the impact of screening and treatment on typhoid fever dynamics in unprotected population, Results Phys., 54 (2023), 11 pages. 1
- [18] R. M. Kaplan, A. Milstein, *Influence of a COVID-19's vaccine's effectiveness and safety profile on vaccination acceptance*, Proc. Natl. Acad. Sci., **118** (2021), 1–5.
- [19] J. P. La Salle, *The stability of dynamical systems*, Society for Industrial and Applied Mathematics, Philadelphia, PA, (1976). 6.2
- [20] Y. A. Liana, J. Z. Ndendya, N. Shaban, *The nutritional nexus: Modeling the impact of malnutrition on TB*, Sci. Afr., **27** (2025), 20 pages. 1
- [21] C. Liu, J. Gao, J. Kanesan, Dynamics analysis and optimal control of delayed SEIR model in COVID-19 epidemic, J. Inequal. Appl., 2024 (2024), 37 pages. 1
- [22] Z. Liu, P. Magal, O. Seydi, G. Webb, A COVID-19 epidemic model with latency period, Infect. Dis. Model., 5 (2020), 323–337. 1
- [23] X. Lu, H.-W. Hui, F.-F. Liu, Y.-L. Bai, Stability and optimal control strategies for a novel epidemic model of COVID-19, Nonlinear Dyn., 106 (2021), 1491–1507. 1
- [24] A. Mahajan, N. A. Sivada, R. Solanki, An epidemic model SIPHERD and its application for prediction of the spread of COVID-19 infection in India, Chaos Solitons Fractals, 140 (2020), 6 pages. 1
- [25] A. K. Misra, J. Maurya, M. Sajid, Modeling the effect of time delay in the increment of number of hospital beds to control an infectious disease, Math. Biosci. Eng., 19 (2022), 11628–11656. 1
- [26] A. Mumbu, J. David, D. Bahaye, J. Ndendya, *Mathematical modeling of culling and vaccination for dog rabies disease transmission with optimal control and sensitivity analysis approach*, Clin. Mol. Epidemiol., **2** (2025), 11 pages. 1
- [27] B. Z. Naaly, T. Marijani, A. Isdory, J. Z. Ndendya, *Mathematical modeling of the effects of vector control, treatment and mass awareness on the transmission dynamics of dengue fever*, Comput. Methods Programs Biomed. Update, **6** (2024), 15 pages. 1
- [28] J. Z. Ndendya, L. Leandry, A. M. Kipingu, A next-generation matrix approach using Routh-Hurwitz criterion and quadratic Lyapunov function for modeling animal rabies with infective immigrants, Healthc. Anal., 4 (2023), 13 pages. 1
- [29] J. Z. Ndendya, Y. A. Liana, A deterministic mathematical model fro conjunctivitis incorporating public health education as a control measure, Model. Earth Syst. Environ., 11 (2025), 17 pages. 1
- [30] J. Z. Ndendya, G. Mlay, H. Rwezaura, *Mathematical modelling of COVID-19 transmission with optimal control and cost-effectiveness analysis*, Comput. Methods Programs Biomed. Update, **5** (2024), 13 pages. 1
- [31] J. Z. Ndendya, E. Mureithi, J. A. Mwasunda, G. Kagaruki, N. Shaban, M. Mayige, Modelling the effects of quarantine and protective interventions on the transmission dynamics of Marburg virus disease, Model. Earth Syst. Environ., 11 (2025), 16 pages. 1
- [32] J. Z. Ndendya, J. A. Mwasunda, S. Edward, N. S. Mbare, A fractional-order model for rabies transmission dynamics using the Atangana-Baleanu-Caputo derivative and MCMC methods, Sci. Afr., 29 (2025), 20 pages. 1
- [33] J. Z. Ndendya, J. A. Mwasunda, N. S. Mbare, Modeling the effect of vaccination, treatment and public health education on the dynamics of norovirus disease, Model. Earth Syst. Environ., 11 (2025), 22 pages. 1
- [34] A. Olivares, E. Staffetti, Optimal control applied to vaccination and testing policies for COVID-19, Mathematics, 9 (2021), 1–22.
- [35] L. S. Pontryagin, V. G. Boltyanskiy, R. V. Gamkrelidze, E. F. Mishchenko, *The mathematical theory of optimal processes*, Interscience Publishers John Wiley & Sons, Inc., New York-London, (1962). 7
- [36] A. Rajput, M. Sajid, Tanvi, C. Shekhar, R. Aggarwal, Optimal control strategies on COVID-19 infection to bolster the

- efficacy of vaccination in India, Sci. Rep., 11 (2021), 18 pages. 1
- [37] A. Senapati, S. Rana, T. Dasi, Chattopadhyay, *Impact of intervention on the spread of COVID-19 in India: a model based study*, J. Theoret. Biol., **523** (2021), 9 pages.
- [38] D. R. Smith, Review a brief history of coronaviruses in Thailand, J. Virol. Methods, 289 (2021), 6 pages. 1
- [39] A. Thongtha, C. Modnak, Optimal COVID-19 epidemic strategy with vaccination control and infection prevention measures in Thailand, Infect. Dis. Model., 7 (2022), 835–855. 2
- [40] A. Vallee, D. Faranda, M. Arutkin, COVID-19 epidemic peaks distribution in the United-States of America, from epidemiological modeling to public health policies, Sci. Rep., 13 (2023), 8 pages. 1
- [41] P. Van den Driessche, J. Watmough, Reproduction number and subthreshold endemic equilibria for compartment models of disease transmission, Math. Biosci., 180 (2002), 29–48. 3.1
- [42] C. Yang, J. Wang, A mathematical model for the novel coronavirus epidemic in Wuhan, China, Math. Biosci. Eng., 17 (2020), 2708–2724.
- [43] B. Yong, J. Hoseana, L. Owen, From pandemic to a new normal: Strategies to optimise governmental interventions in Indonesia based on an SVEIQHR-type mathematical model, Infect. Dis. Model., 7 (2022), 346–363. 2
- [44] S. Zhao, H. Chen, Modeling the epidemic dynamics and control of COVID-19 outbreak in China, Quant. Biol., 8 (2020), 11–19. 1